QED RADIATIVE CORRECTIONS, MONTE CARLO AND SPIN; THE CASE OF τ-PAIR PRODUCTION IN e^+e^- ANNIHILATION*

By S. Jadach

Institute of Physics, Jagellonian University, Cracow**

(Received March 27, 1985)

It is shown how to combine Monte Carlo techniques with methods based on spin amplitudes in order to calculate radiatively corrected, integrated, and/or differential QED cross sections efficiently for heavy lepton τ production in an electron-positron annihilation process. A particular emphasis is put on those aspects which are potentially important for future developments for this process, for applications to similar processes (production of heavy quarks), and for other QED processes where mass and spin effects are also important (in addition to the radiative ones).

PACS numbers: 12.20.Ds

1. Introduction

Over the last two decades, from the joint efforts of experimental and theoretical physicists, a new picture of fundamental interactions and constituents in Particle Physics has emerged, in which interactions are mediated by gauge bosons from a $SU(3)_{colour} \otimes SU(2) \otimes U(1)_{electroweak}$ group [1–4], and elementary constituents are leptons and quarks, grouped into three families.

Much of the experimental information which contributed to formulating this, by now, Standard Theory of Particle Interactions (STPI) comes from electron-positron scattering experiments. For example the first two members of the third family, the heavy lepton τ and heavy quark b, were found in experiments of that type. See Ref. [5] and references there for a review of e^+e^- experimental results.

Although STPI has in principle an enormous predictive power due to its renormalizability [6], at this moment however, even its basic assumptions, like universality of coupling constants in the fermion sector and gauge nature of the intermediate heavy bosons, are far from being fully tested, while verification of predictions based on its renormalizability

* This paper is presented as the qualifying thesis for habilitation at Jagellonian University, Cracow.

** Address: Instytut Fizyki UJ, Reymonta 4, 30-059 Kraków, Poland.

is still confined to its quantum-electrodynamical (QED) sector[1]. The e^+e^- scattering experiments are generally much cleaner than experiments with hadron beams or targets, simply because the elementary constituents — quarks — are confined in hadrons. This is the reason why experiments with e^+e^- intersecting beams are anticipated to be the best place for precise tests of STPI in the future [7].

Currently, the experiments of this type are continuously supplying valuable data on properties of quarks and leptons, on Z_0 coupling constants and on high energy behaviour of typical QED processes. The data on QED processes ranging from the simple annihilation process $e^+e^- \to \bar{f}f$, f = quark, lepton, to such processes as $e^+e^- \to \bar{f}f\gamma\gamma$ or $e^+e^- \to \bar{f}f\bar{f}'f'\gamma$ are analyzed in present experiments from two points of view. Either they are objects of interest in themselves, or they are regarded as an unwanted background while analyzing data or looking for some other process.

In the first case, the agreement (until now) of the experimental data with the perturbative QED calculations is regarded as a further confirmation of this oldest and most solid sector of renormalizable STPI, and as a proof of the pointlike nature of fundamental constituents up to the shortest measurable distances.

In the second case, the QED effects play the role of the known and uninteresting component which has to be subtracted from the data. For example the $O(\alpha^3)$ QED contribution for forward-backward asymmetry in $e^+e^- \to \mu^+\mu^-$ process is subtracted from the data [5] to isolate a pure Z_0 contribution. In searches for new exotic particles, the QED bremsstrahlung at large angles is considered as a background.

In any case, it is rather obvious that, for the purpose of present/future e^+e^- experiments, there is a great necessity to calculate the differential cross sections (final state distribution), event rates etc. for a wide range of the QED/STPI processes, both at the three level and with higher order radiative (perturbative) corrections.

There exist, of course, forty years old techniques for calculating QED distributions which include Feynman rules, renormalization prescriptions for removing divergences (order by order) and methods for summing over spins. They prove, however, when confronted by the demands of present e^+e^- experiments, to be incomplete and/or inadequate quite often. The problems which arise are of a purely technical nature, and are generally related to the presence of three and more particles in the final state. The inclusion of more than two particles in the final state has two important consequences: first, a proliferation of the Feynman diagrams; and second, a need to integrate exactly over five and higher dimensional phase space.

The first problem may be seen by comparing the processes $e^+e^- \to e^+e^-$ and $e^+e^- \to e^+e^-e^+e^-$. The first one has two Feynman diagrams which yield 4 terms in the differential cross section. In the second case 36 diagrams yield 1296 terms. In this and other processes, when standard techniques are used, one is faced with an *avalanche* of the long *algebraic* expressions which are difficult to control and to understand. Without entering into details, I indicate only that a solution of this first problem is found using spin amplitudes and related methods.

---

[1] Usually I omit from discussion the $SU(3)_{colour}$ sector.

The problem of integrating exactly over a complete multiparticle final state, in the traditional QED calculations, was somehow avoided by the use of all sorts of "effective photon", "soft photon" etc. approximations [8]. The growing precision of experiments and the interest in the large transverse momenta events created the necessity of taking into account the complete final state phase space. Similar problems arose in late sixties in multihadron production by strong interactions, and were successfully solved by a use of Monte Carlo (M.C.) methods [9]. There are, however, important differences between multiparticle production in the old days and present QED processes.

In the multihadron production one could use universal phase space integration programs [9] for a wide range of processes and final states. In QED the distributions are more complicated, and they have very strong peaks and/or singularities in the phase space. An efficient M.C. algorithm (program) has to be prepared individually for every QED process and its construction may be rather laborious.

Another difference comes from the experimental side. Due to an evolution of experimental techniques (electronic experiments instead of bubble chambers) there is, now, a strong pressure to present the predictions of theory for a given scattering process not in a form of formulae and tables, but rather in a form of a M.C event generator which simulates the scattering process directly. The analysis of experimental data from modern detectors relies heavily on an elaborate M.C. simulation of the detector. If the M.C. event generator, based on a theoretical model, is available, then all the detector effects (triggers, acceptance, resolution, etc.) can be taken into account, while comparing theory with experiment, in a natural and simple way: the event generator (based on theory) is plugged in, as a first step in a (usually larger) M.C. type program which simulates the detector behaviour. Also the additional selection criteria used in the data analysis (all sorts of cut-offs) can be introduced in such M.C. simulation in the same way as in the real data analysis i.e. by rejecting some of the M.C. events.

In this paper I review methods of calculating QED distributions and of the M.C. integration over the final state momenta for the combined τ production and decay process [10, 11]

$$e^+e^- \to \tau^+\tau^-(\gamma), \quad \tau^\pm \to X^\pm. \tag{1.1}$$

As compared with other QED processes, this process has its own specific character and technical problems to solve which may be summarized as follows:

(A) The lepton τ is unstable, and is observed at present only through its decay products [12]. The differential cross section for process (1.1) does not factorize into production and decay parts, because the τ decay is sensitive to its spin polarization. The above distribution, when calculated with traditional trace techniques, consists of rather long algebraic expressions even in the QED lowest order, $O(\alpha^2)$ [13, 14]. The situation deteriorates strongly when radiative effects (keeping finite τ mass) are included. Note that in this case the source of the "algebraic avalanche" is not in the multitude of Feynman diagrams, although this will be the case when the Z_0 contribution is taken in its full form, but rather is in the spin structure, the nonzero mass of the τ, and the necessity of including the decay of the τ.

(B) The use of the M.C. integration method for the final state phase space in (1.1)

is practically unavoidable due to the presence of at least four (typically 5–8) particles in the final state.

(C) There is no single dominant τ decay mode [15]. The decay part in (1.1) should be treated as *exchangeable* in the calculations, i.e. it should be easy to replace one decay mode by another without any intervention in the radiatively corrected production part in (1.1). This constraint is rather important, and in practice it means that the spin structure in the calculations of the distributions for (1.1) (and in the M.C. algorithm) must be organized in such a way that the production and decay parts in (1.1) are separated as strongly as possible.

The problems (A)–(C) were solved successfully in Refs [10] and [11]. In Ref. [10] the $O(\alpha^3)$ QED spin amplitudes for production process $e^+e^- \to \tau^+\tau^-(\gamma)$ were calculated, and methods of calculating the differential cross section for the combined process (1.1) in a way assuring condition (C) were given. In Ref. [11] the M.C. program for (1.1) is described in every detail. Ref. [10] contains also the quantitative discussion of radiative and spin effects for (1.1) in the energy range $2m_\tau \leqslant \sqrt{s} \leqslant 40$ GeV based on numerical M.C. results.

In this work, I do not attempt to reproduce all the results of Refs [10] and [11], but I rather concentrate on those topics which were not fully covered in those papers, and I reformulate and generalize the techniques, developed there, which, in the future, may find applications in other QED/STPI processes, or for (1.1) at higher energies.

I concentrate mainly on two subjects: (I) The techniques for calculating the differential cross (d.c.) section for annihilation of polarized e^+e^- into a pair of heavy unstable fermions (leptons, quarks). (II) The general methods of constructing Monte Carlo algorithms individually adapted (IAMC) to a given distribution and their applications to process (1.1), and to other similar QED processes.

Elaborating on subject (I) I define all ingredients necessary for calculating the d.c. section for process (1.1), i.e. spin states, techniques of calculating spin amplitudes and methods of evaluating numerically the d.c. section out of spin amplitudes. Following Refs [16] and [17] first, the spin amplitudes are calculated analytically and then also numerically for every Feynman diagram (or for gauge invariant groups of them), and afterwards the transition from the spin amplitudes to the d.c. section (including summation over Feynman diagrams) is done not analytically (as in traditional methods), but rather also *numerically*. In this way, taking advantage of the relative simplicity of spin amplitudes, one eliminates the source of the "algebraic avalanche" in the d.c. section, mentioned earlier in that Section. This partly analytical and partly numerical method, based on spin amplitudes (ANSA) was used in Refs [10], [11], for process (1.1) with polarized $e^\pm$ and decaying $\tau^\pm$. A similar method was also used in Refs [16] and [17] for the four lepton production process $e^+e^- \to l^+l^-l^+l^-$, with all leptons almost massless ($l = e, \mu$) unpolarized and stable.

Subject (II) includes a systematic review of the IAMC methods. As was pointed out, the problem of constructing a M.C. event generator for a QED scattering process is equivalent to finding an efficient method of generating random points precisely according to a given, multidimensional, complicated and strongly peaked distribution. The above

task is known to be difficult, laborious, and cannot be done without a detailed knowledge of all the properties of the distribution in question. Literature on this specific subject is rather scarce, and one tends to believe that finding an efficient IAMC algorithm is entirely a matter of art and experience. I shall try to show, however, that in a typical IAMC algorithm one employs in fact only a few basic methods. They are used in a recursive way such that, ultimately, the generation of a multidimensional complicated distribution is reduced to a series of generations of less dimensional, often one dimensional, simple distributions. This rather detailed discussion of the IAMC techniques is introduced for the purpose of the process (1.1) and other QED processes, although they apply as well to many other non-QED problems. It is shown in more detail how those basic IAMC methods were used to construct the M.C. algorithms for process (1.1) and $e^+e^- \to \mu^+\mu^-(\gamma)$ $(e^+e^- \to \bar{q}q(\gamma))$.

The outline of the paper is the following: In Section 2 I define spin states and density matrix formalism for process (1.1) in a way assuring separation of production and decay parts, and such that the calculations of QED spin amplitudes for (1.1) demonstrated in Section 3 are relatively simple. In Section 4 I review IAMC methods in general terms (for arbitrary distributions), and in Section 5 I describe how they were used for the τ production and decay process (1.1). Comparisons with other M.C. programs $(e^+e^- \to \mu^+\mu^-(\gamma))$ and future extensions are also discussed in Section 5.

2. From spin amplitudes to differential cross section

In the second part of ANSA techniques, which was sketched in the Introduction, the differential cross section of the scattering process is calculated numerically out of spin amplitudes. In this Section I concentrate on the question of defining spin states and spin amplitudes for the τ production process

$$e^+(p_1)+e^-(p_2) \to \tau^+(q_1)+\tau^-(q_2)+(\gamma(k)), \tag{2.1}$$

and then, on the problem of evaluating the final state d.c. section, taking polarized $e^\pm$ and $\tau^\pm$ decays sensitive to their polarizations. Possible generalizations of the methods presented will be also commented upon.

The algebraic complexity of spin amplitudes depends strongly on the appropriate choice of the spin states and kinematic variables. A choice presented in this Section suits best the process (2.1) with the *s*-channel annihilation photon, and other similar ones. This will become more evident in the next Section where examples of practical calculations of the spin amplitudes will be shown.

Calculating final state distributions in the case of unpolarized incident particles, and spin-insensitive detection of outgoing particles, merely amounts to taking the sum of modulus-squares of all spin amplitudes (summed over Feynman diagrams). In the case of polarized particles, and spin sensitive detection, the standard technique is to use the spin density matrices. In the second part of this Section it will be shown how to define and to use spin density matrices for $e^\pm$ and, as well, for a decaying $\tau^\pm$, in a way suitable for the M.C. type calculations.

Spin states

I define spin states of $e^{\pm}$ and $\tau^{\pm}$ in the rest frame of the corresponding fermion, denoted by $RS_1(e^{\pm})$ and/or $RS(\tau^{\pm})$, as a state with a definite spin projection on the third axis. These fermion rest frames are connected to an overall center of mass (laboratory) system CMS by Lorentz transformations $L_t(e^{\pm})$ and $L_t(\tau^{\pm})$, where $t = 0$ ($t = 1$) indicates that a hard bremsstrahlung photon is absent (present). The transformations L_t are parametrized in terms of angles and boost velocities which also serve as the independent kinematical variables parametrizing the spin amplitudes and the phase space integral simultaneously.

Definitions of spin states (polarization vectors) of the hard bremsstrahlung photon (also connected to L_t) will be given later in this Section.

The complete list of the definitions of the spin states for $e^{\pm}$ and $\tau^{\pm}$ in the process (2.1) is the following:

$$
\begin{aligned}
|e^+; p_1, \lambda_1\rangle &= U(L_t(e^+))\,|e^+; \mathring{p}, \lambda_1\rangle,\\
|e^-; p_2, \lambda_2\rangle &= U(L_t(e^-))\,|e^-; \mathring{p}, \lambda_2\rangle,\\
|\tau^+; q_1, \alpha_1\rangle &= U(L_t(\tau^+))\,|\tau^+; \mathring{q}, \alpha_1\rangle,\\
|\tau^-; q_2, \alpha_2\rangle &= U(L_t(\tau^-))\,|\tau^-; \mathring{q}, \alpha_2\rangle,\\
p_1 &= L_t(e^+)\mathring{p}, \qquad p_2 = L_t(e^-)\mathring{p},\\
q_1 &= L_t(\tau^+)\mathring{q}, \qquad q_2 = L_t(\tau^-)\mathring{q},\\
\mathring{p} &= (m, 0, 0, 0), \qquad \mathring{q} = (M, 0, 0, 0),\\
L_0(e^{\pm}) &= R_3(\varphi)B_3(\pm\eta_e),\\
L_0(\tau^{\pm}) &= R_3(\varphi)R_1(-\theta)B_3(\pm\eta_\tau),\\
L_1(e^{\pm}) &= R_3(\varphi_1)B_3(\pm\eta_e),\\
L_1(\tau^{\pm}) &= R_3(\varphi_1)R_1(-\theta_1)B_3(-\zeta)R_3(\varphi_2)R_1(-\theta_2)B_3(\pm\eta_\tau).
\end{aligned}
\tag{2.2}
$$

The above definitions are, in spirit, quite similar to definitions of the standard helicity states [18]. The states $|e^{\pm}; \mathring{p}, \lambda\rangle$ and $|\tau^{\pm}; \mathring{q}, \alpha\rangle$ represent, here, $e^{\pm}$ and $\tau^{\pm}$ in their rest frames ($RS_1(e^{\pm})$, $RS(\tau^{\pm})$) with spin projections $\lambda, \alpha = \pm 1/2$ on the third axis. The unitary matrix $U(L_t)$ represents the Lorentz transformation L_t for $e^{\pm}$, $\tau^{\pm}$ lepton. (In the calculations of the spin amplitudes from Feynman rules the states $|e; p, \lambda\rangle$, $|\tau; q, \alpha\rangle$ will be

Fig. 1. Kinematics of the a) $e^+e^- \to \tau^+\tau^-$, b) $e^+e^- \to \tau^+\tau^-\gamma$ processes. Boxes represent reference systems. They are connected by Lorentz transformations marked on arrows. Most important reference frames are: the laboratory reference system CMS, the rest system of the $\tau^+\tau^-$ pair QMS, te rest systems of $\tau^{\pm}$ leptons $RS(\tau^{\pm})$ used to quantize $\tau^{\pm}$ spins and to simulate $\tau^{\pm}$ decays in the M. C. algorithm, and the $e^{\pm}$ rest systems $RS(e^{\pm})$, where the $e^{\pm}$ polarization vectors are defined. Other intermediate systems are used for calculating spin amplitudes, to define polarization vectors of emitted photon, etc.

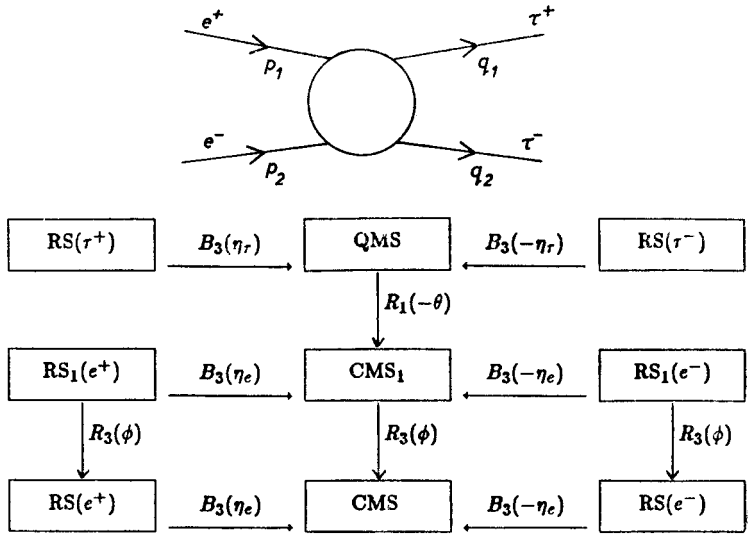
e^+
p_1
τ^+
q_1
e^-
p_2
τ^-
q_2
RS(τ^+)
$B_3(\eta_\tau)$
QMS
$B_3(-\eta_\tau)$
RS(τ^-)
$R_1(-\theta)$
RS$_1$(e^+)
$B_3(\eta_e)$
CMS$_1$
$B_3(-\eta_e)$
RS$_1$(e^-)
$R_3(\phi)$
$R_3(\phi)$
$R_3(\phi)$
RS(e^+)
$B_3(\eta_e)$
CMS
$B_3(-\eta_e)$
RS(e^-)

Fig. 1a

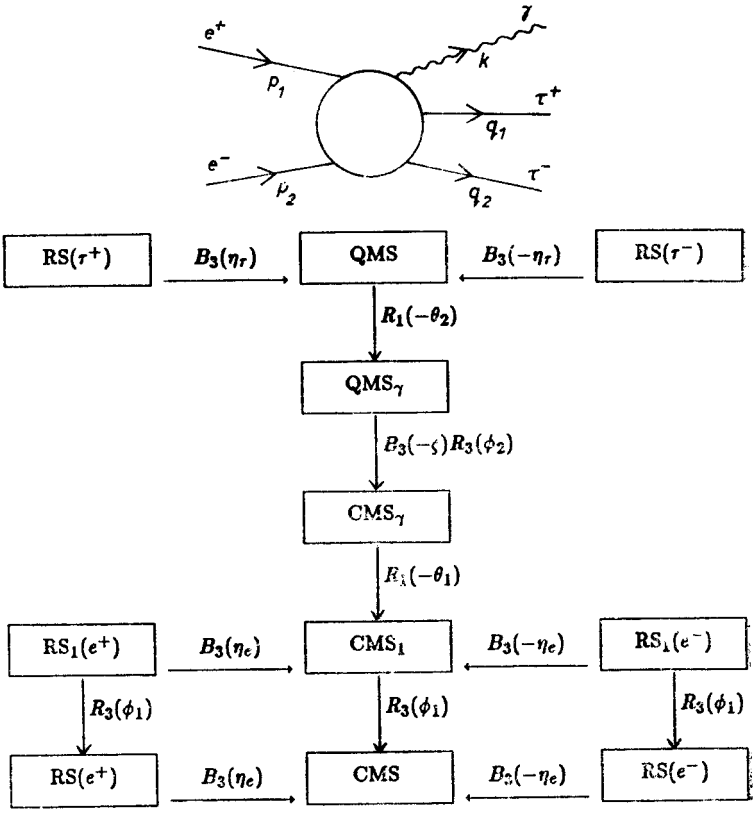
e^+
p_1
γ
k
τ^+
q_1
e^-
p_2
τ^-
q_2
RS(τ^+)
$B_3(\eta_\tau)$
QMS
$B_3(-\eta_\tau)$
RS(τ^-)
$R_1(-\theta_2)$
QMS$_\gamma$
$B_3(-\zeta)R_3(\phi_2)$
CMS$_\gamma$
$R_1(-\theta_1)$
RS$_1$(e^+)
$B_3(\eta_e)$
CMS$_1$
$B_3(-\eta_e)$
RS$_1$(e^-)
$R_3(\phi_1)$
$R_3(\phi_1)$
$R_3(\phi_1)$
RS(e^+)
$B_3(\eta_e)$
CMS
$B_3(-\eta_e)$
RS(e^-)

Fig. 1b

effectively replaced by the corresponding Dirac spinors and $U(L_t)$ by matrix $S(L_t)$ acting on spinors.) The transformations L_t are shown in a graphical way in Fig. 1 together with reference systems $RS_1(e^{\pm})$, $RS(\tau^{\pm})$, CMS, and other intermediate reference frames, which are obtained by truncation of the chain of boosts and rotations in L_t. The transformation $B_3(\pm\eta_\tau)$ is a boost transformation along the third axis, where

$$B_3(\eta) = \begin{bmatrix} \cosh\eta & 0 & 0 & \sinh\eta \\ 0 & 1 & 0 & 0 \\ 0 & 0 & 1 & 0 \\ \sinh\eta & 0 & 0 & \cosh\eta \end{bmatrix}, \tag{2.3}$$

and it relates the $\tau^{\pm}$ rest frame $RS(\tau^{\pm})$ with the rest frame of the $\tau^{\pm}$ pair denoted as QMS. A similar role is played by $B_3(\pm\eta_e)$. The velocities η_e, η_τ are related to momenta products;

$$p_1 \cdot p_2 = m^2 \cosh 2\eta_e, \quad q_1 \cdot q_2 = M^2 \cosh 2\eta_\tau, \tag{2.4}$$

where m and M are masses of electron and τ. In the radiative case ($t = 1$) the $\tau^{\pm}$ pair rest frame QMS_γ and $e^{\pm}$ pair rest frame CMS_γ, see Fig. 1b, are related by a boost $B_3(-\zeta)$ along the photon momentum; note that $k = p_1+p_2-q_1-q_2$. The velocity ζ in this boost may be obtained from

$$\cosh\zeta = (q_1+q_2)\cdot(p_1+p_2)\,((p_1+p_2)^2\,(q_1+q_2)^2)^{-1/2}. \tag{2.5}$$

The meaning of the angles θ, φ, θ_i, φ_i, looking at definitions of L_t and at Fig. 1, is self explanatory. The angles θ, φ are angular variables of the $\tau^{\pm}$ in CMS (in the nonradiative case). Since photon momentum is parallel to the third axis in CMS_γ and QMS_γ, the angles θ_1, φ_1 are angular variables of the photon in CMS, θ_2 is an angle between photon and $\tau^{\pm}$ in $\tau^{\pm}$ pair system QMS, and φ_2 is an angle between two planes; one spanned on vectors $(\vec{p}_1, \vec{p}_2, \vec{k})$ and another on $(\vec{q}_1, \vec{q}_2, \vec{k})$.

The momenta of $e^{\pm}$ and $\tau^{\pm}$ can be expressed in terms of the angles and boost velocities in any of the reference systems in Fig. 1 by taking $\mathring{p}$ or $\mathring{q}$ and applying the appropriate transformations, read from Fig. 1. The momentum of the photon is parallel to third axis in CMS_γ

$$\{k^\mu\}_{CMS_\gamma} = 2^{-1}s^{1/2}(k, 0, 0, k), \tag{2.6}$$

where $k = 1-\exp(-2\zeta)$ is the CMS photon momentum in units of the beam energy $E = 2^{-1}s^{1/2}$.

In CMS the photon momentum reads

$$k_{CMS} = R_1(-\theta_1)R_3(\varphi_1)k_{CMS_\gamma}$$

$$= E(k, -k\sin\theta_1\sin\varphi_1, k\sin\theta_1\cos\varphi_1, k\cos\theta_1). \tag{2.7}$$

The CMS_γ frame is also used to define two transverse polarizations of the bremsstrahlung photon as

$$CMS_\gamma: \varepsilon^\mu_{(\beta)} = \delta^\mu_\beta, \quad \text{for} \quad \beta = 1, 2. \tag{2.8}$$

This choice is particularly convenient for calculations of spin amplitudes for the initial state bremsstrahlung. For the final state bremsstrahlung, another, analogous choice, $\varepsilon'^\mu_{(\beta)} = \delta^\mu_\beta$ in QMS_γ, yields simpler spin amplitudes. The above two sets are related by a rotation $R_3(\varphi_2)$.

Finally, the phase space integral may also be expressed in terms of the same variables which parametrize transformations L_t;

$$d\tau_2 = \delta^4(p_1+p_2-q_1-q_2)\frac{d^3q_1 d^3q_2}{q_1^0 q_2^0} = \tfrac{1}{2}\,\mathrm{tgh}\,\eta_e d\cos\theta d\varphi,$$

$$d\tau_3 = \delta^4(p_1+p_2-q_1-q_2-k)\frac{d^3q_1}{q_1^0}\frac{d^3q_2}{q_2^0}\frac{d^3k}{k^0}$$

$$= \tfrac{1}{2}E^2\,\mathrm{tgh}\,\eta_e\,\mathrm{thg}\,\eta_\tau k dk\, d\cos\theta_1 d\varphi_1 d\cos\theta_2 d\varphi_2. \tag{2.9}$$

The advantages of the above choice of spin states and kinematics will become more obvious in the following Sections, while calculating spin amplitudes and constructing M.C. algorithms. Here, I indicate only some of them: Due to the fact that the reference frames $RS_1(e^\pm)$ and $RS(\tau^\pm)$ are rigidly tied to particle momenta the spin amplitudes do not depend on the azimuthal angles φ, φ_1. This dependence is restored by rotation of the polarization vectors from $RS(e^\pm)$ to $RS_1(e^\pm)$ and of the photon polarizations from QMS_γ to CMS_γ.

Generally, the above choice of spin states simplifies spin amplitudes for the s-channel e^+e^- annihilation process plus bremsstrahlung from every initial/final state fermion. The important thing is that the leading singularities (from bremsstrahlung propagators) are, with this choice of variables, easily detected and isolated for an individual treatment (in M.C.). This is closely related to the fact that one of the boosts in L_t (between CMS_γ and QMS_γ) is along the photon momentum.

Spin amplitudes and differential cross section

In the following I define spin amplitudes and I introduce a density matrix formalism using as an example, but without loss of generality, the nonradiative case of τ production and decay process.

Spin amplitudes in this case ($t = 0$) are constructed using spin states from Eqs (2.2) as follows

$$\mathcal{M}^0_{\lambda_1\lambda_2\alpha_1\alpha_2} = \langle\alpha_1\alpha_2|M^0(e^+e^- \to \tau^+\tau^-)\,|\lambda_1\lambda_2\rangle, \tag{2.10}$$

where

$$|\lambda_1\lambda_2\rangle = |e^+;\, p_1, \lambda_1\rangle \otimes |e^-;\, p_2, \lambda_2\rangle,$$

$$|\alpha_1\alpha_2\rangle = |\tau^+;\, q_1, \alpha_1\rangle \otimes |\tau^-;\, q_2, \alpha_2\rangle.$$

With this choice of spin states, they are Lorentz invariant in the same sense as the conventio-

nal helicity amplitudes. This is due to the fact that the reference frames $RS_1(e^{\pm})$ and $RS(\tau^{\pm})$ are rigidly attached to particle momenta.

The d.c. section for polarized particles may be expressed in terms of spin amplitudes and density matrices,

$$d\sigma = 4 \sum \sum_{\substack{\lambda_i\bar{\lambda}_i \\ \alpha_i\bar{\alpha}_i}} \varrho^{(1)}_{\lambda_1\bar{\lambda}_1}\varrho^{(2)}_{\lambda_2\bar{\lambda}_2}\mathcal{M}^0_{\lambda_1\lambda_2\alpha_1\alpha_2}(\mathcal{M}^0_{\bar{\lambda}_1\bar{\lambda}_2\bar{\alpha}_1\bar{\alpha}_2})^*\pi^{(1)}_{\bar{\alpha}_1\alpha_2}\pi^{(2)}_{\bar{\alpha}_2\alpha_2}d\tau_2, \tag{2.11}$$

where

$$\varrho^{(i)} = \tfrac{1}{2}(I + \vec{\sigma}\cdot\vec{\varepsilon}_i) = \tfrac{1}{2}\sum_{a=0}^{3}\sigma^a\tilde{\varepsilon}^a_{(i)},$$

$$\pi^{(i)} = \tfrac{1}{2}(I + \vec{\sigma}\cdot\vec{\chi}_i) = \tfrac{1}{2}\sum_{a=0}^{3}\sigma^a\tilde{\chi}^a_{(i)}, \tag{2.12}$$

and σ^i, $i = 1, 2, 3$ are Pauli matrices supplemented with $\sigma^0 = I$. The spin density matrices $\varrho^{(i)}$ are, in a standard way, parametrized by spin polarization vectors $\vec{\varepsilon}_i$ defined in $e^{\pm}$ rest frames ($RS_1(e^{\pm})$). The vectors $\vec{\chi}_i$, defined in $RS(\tau^{\pm})$, are not strictly speaking the polarization vectors of the $\tau^{\pm}$, but rather they characterize an experimental device (a polarimeter) measuring polarization of the $\tau^{\pm}$. The meaning of $\vec{\chi}_i$ will become more clear later, when the decay of the $\tau^{\pm}$, playing a role of such a polarimeter, is included in the discussion. Vectors $\tilde{\varepsilon}_{(i)} = (1, \vec{\varepsilon}_i)$ and $\tilde{\chi}_{(i)} = (1, \vec{\chi}_i)$ are introduced to make the notation more compact, and they are only defined in the corresponding fermion rest frames.

Vector parametrization for $\varrho^{(i)}$ and $\pi^{(i)}$ is introduced because of the known advantages of the polarization vectors. They transform more easily under rotation, the case of unpolarized particles is defined in a simple way ($\vec{\varepsilon} = 0$), and they are more directly related to experimental measurables (angular distributions). Their properties are also useful in the M.C. calculations. The concept of a polarization vector, preserving all the above virtues, may be generalized to higher spins, see Appendix A and references there.

The distribution (2.11) in a vector notation reads as follows

$$d\sigma = \sum_{abcd=0}^{3}\tilde{\varepsilon}^a_{(1)}\tilde{\varepsilon}^b_{(2)}R_{abcd}\tilde{\chi}^c_{(1)}\tilde{\chi}^d_{(2)}d\tau_2, \tag{2.13}$$

where

$$R_{abcd} = \sum_{\alpha_i\bar{\alpha}_i}\sum_{\lambda_i\bar{\lambda}_i}\sigma^a_{\lambda_1\bar{\lambda}_1}\sigma^b_{\lambda_2\bar{\lambda}_2}\mathcal{M}^0_{\lambda_1\lambda_2\alpha_1\alpha_2}(\mathcal{M}^0_{\bar{\lambda}_1\bar{\lambda}_2\bar{\alpha}_1\bar{\alpha}_2})^*\sigma^c_{\bar{\alpha}_1\alpha_1}\sigma^d_{\bar{\alpha}_2\alpha_2}. \tag{2.14}$$

The elements of tensor R have a direct physical meaning; R_{0000} is the spinless d.c. section, $d\sigma_{unp}/d\tau_2 = R_{0000}$, the polarization vector of τ^+ (for unpolarized $e^{\pm}$) is given by $s_i = R_{00i0}/R_{0000}$, the spin correlation tensor for $\tau^{\pm}$ pair is found to be $r_{ab} = R_{00ab}/R_{0000}$ [10] etc.

Let us, now, include in the discussion the decays of the $\tau^{\pm}$. The normalized (to unity) decay probability distribution $dp^{(i)}$ for polarized τ^+ ($i = 1$) or τ^- ($i = 2$) reads

$$dp^{(i)} = \varrho'^{(i)}_{\alpha_i\bar{\alpha}_i}\mathcal{M}_{\alpha_i}(\mathcal{M}_{\bar{\alpha}_i})^*d\tau^{(i)}_{dec}, \tag{2.15}$$

where $\varrho'^{(i)} = 2^{-1}(I+\vec{\sigma}\cdot\vec{w}_i)$ is the spin density matrix of the $\tau^\pm$, and $\vec{w}_i$ is its polarization vector. Spin amplitudes

$$\mathcal{M}^{(i)}_{\alpha_i} = \langle X^\pm | M(\tau^\pm \to X^\pm) | \tau^\pm; q_i, \alpha_i\rangle \tag{2.16}$$

describe the decay of the $\tau^\pm$. The phase space e'ement $d\tau^{(i)}_{\text{dec}}$ is assumed to include information on momenta and spin of decay products and an energy momentum conservation δ-function.

The distribution (2.15) in vector notation reads

$$dp^{(i)} = \sum_{a=0}^{3} \tilde{w}^a H^a_{(i)} d\tau^{(i)}_{\text{dec}}, \qquad \tilde{w} = (1, \vec{w}), \tag{2.17}$$

where

$$H^a_{(i)} = \sum_{\alpha\bar{\alpha}} \sigma^a_{\alpha\bar{\alpha}} \mathcal{M}^{(i)}_{\alpha} (\mathcal{M}^{(i)}_{\bar{\alpha}})^*. \tag{2.18}$$

For the combined production plus decay process $e^+e^- \to \tau^+\tau^-$, $\tau^\pm \to X^\pm$ spin amplitudes multiply directly

$$\mathcal{M}^{\text{comb}}_{\lambda_1\lambda_2} = \sum_{\alpha_1\alpha_2} \mathcal{M}^0_{\lambda_1\lambda_2\alpha_1\alpha_2} \mathcal{M}^{(1)}_{\alpha_1} \mathcal{M}^{(2)}_{\alpha_2} \tag{2.19}$$

and the d.c. section reads

$$d\sigma = \varrho^{(1)}_{\lambda_1\bar{\lambda}_1} \varrho^{(2)}_{\lambda_2\bar{\lambda}_2} \mathcal{M}^{\text{comb}}_{\lambda_1\lambda_2} (\mathcal{M}^{\text{comb}}_{\bar{\lambda}_1\bar{\lambda}_2})^* d\tau_2 d\tau^{(1)}_{\text{dec}} d\tau^{(2)}_{\text{dec}}. \tag{2.20}$$

In M.C. calculations, the formulae (2.19), (2.20) are not very handy, because production and decay parts are not clearly separated. This separation becomes more manifest in vector notation [11]

$$d\sigma = \sum_{abcd=0}^{3} \tilde{\varepsilon}^a_{(1)} \tilde{\varepsilon}^b_{(2)} R_{abcd} H^c_{(1)} H^d_{(2)} d\tau_2 d\tau^{(1)}_{\text{dec}} d\tau^{(2)}_{\text{dec}}. \tag{2.21}$$

By comparing Eqs (2.13) and (2.12) we may see the meaning of the vectors $\vec{\chi}_i$ for the decaying $\tau^\pm$. They should be identified with the vectors $\vec{h}_{(i)}$ defined as

$$h^k_{(i)} = H^k_{(i)}/H^0, \qquad k = 1, 2, 3,$$

and they characterize the efficiency of a given τ decay as a polarimeter. In Ref. [10] vectors $\vec{h}$ are listed for typical one prong τ decays.

A few remarks on the presented spin formalism are in order. First is its relation to the standard QED technique based on spin projection operators [7]

$$\Lambda_\pm(p, s) = (\not{p} + m)(I + \gamma_5 \not{s})/2. \tag{2.22}$$

As expected, see also Ref. [10], they are equivalent. Tensors R_{abcd} and $H^a_{(i)}$ may be calculated either from spin amplitudes, as in (2.14) and (2.18), or using operators (2.22). For example the τ decay probability distribution in its rest frame, calculated using (2.22), may be always written in form (2.17), with a term linear in $\vec{s}$ and a constant. The corresponding coefficients are identified with $\vec{H}$ and H^0. In principle the same method may be used to calculate R_{abcd} and in fact was used in Ref. [10] to obtain R_{00cd} for certain numerical tests.

The inclusion of the radiative photon in the presented formalism is rather trivial. Since one is not interested in its polarization, a summation over two transverse photon polarizations should be included in the formula (2.14) for R_{abcd}, and the phase space element $d\tau_2$ in (2.21) should be replaced by $d\tau_3$ if necessary. The infrared divergences do not cancel out for spin amplitudes, but rather in the tensor R_{abcd}, and the contributions $O(\alpha^4)$ in (2.14) are neglected.

Generalizations

The above formalism generalizes easily to more particles in the final state, to higher spins and to sequential decays. It applies in a rather straightforward way to t-quark production process $e^+e^- \to \vec{t}t(\gamma)$, $\vec{t} \to$ jets. Spin effects in the final state may not be negligible in this process.

An interesting application of this formalism is the $W^\pm$ pair production process $e^+e^- \to W^+W^-(\gamma)$. As in the τ production case, $W^\pm$ are visible only through their decay products, and $W^\pm$ decays are strongly sensitive to $W^\pm$ polarizations. Radiative effects, mass effects and spin effects will be of similar size. The formula (2.21) generalizes in this case as follows:

$$d\sigma = \sum_{ab=0}^{3} \sum_{J_i=0}^{2} \sum_{M_t=-J_t}^{J_t} \tilde{\varepsilon}^a_{(1)} \tilde{\varepsilon}^b_{(2)} R_{ab M_1 M_2}^{J_1 J_2} d\tau_{\text{prod}} \times H_{(1)M_1}^{J_1} d\tau_{\text{dec}}^{(1)} H_{(2)M_2}^{J_2} d\tau_{\text{dec}}^{(2)}, \tag{2.23}$$

where the tensor R is calculated out of spin amplitudes $\mathcal{M}_{\lambda_1\lambda_2\alpha_1\alpha_2\beta}$ for $e^+e^- \to W^+W^-(\gamma)$ as follows:

$$R_{ab M_1 M_2}^{J_1 J_2} = \sum_{\lambda_i \bar{\lambda}_i} \sum_{\alpha_i \bar{\alpha}_i \beta} \sigma^a_{\lambda_1 \bar{\lambda}_1} \sigma^b_{\lambda_2 \bar{\lambda}_2} \mathcal{M}_{\lambda_1\lambda_2\alpha_1\alpha_2\beta} \times (\mathcal{M}_{\bar{\lambda}_1\bar{\lambda}_2\bar{\alpha}_1\bar{\alpha}_2\beta})^* Z^{J_1}_{M_1, \bar{\alpha}_1\alpha_1} Z^{J_2}_{M_2, \bar{\alpha}_2\alpha_2}, \tag{2.24}$$

see Appendix A for definition of $Z^J_{M,\bar{\alpha}\alpha}$.

The tensor $H_{(i)M}^{J}$ characterizes the decay probability distribution

$$dp_{(i)}(W^\pm \to X^\pm) = \sum_{JM} t^J_M H_{(i)M}^{J} d\tau_{\text{dec}}^{(i)}, \tag{2.25}$$

see Eq. (2.11), where $W^\pm$ is polarized according to tensor t^J_M, see Appendix A.

The example of the sequential decay $e^+e^- \to \tau^+\tau^-(\gamma)$, $\tau^+ \to X^+$, $\tau^- \to \nu\varrho^-$, $\varrho^- \to \pi^+\pi^0$ will be discussed in Section 5 and in Appendix A.

3. Calculating spin amplitudes

In this Section I show a few examples of practical calculations of the QED spin amplitudes for the τ pair production process (without decay). These methods apply directly to the production of other heavy fermion pairs, $e^+e^- \to \bar{f}f(\gamma)$. They may also be generalized to the case of the double bremsstrahlung $e^+e^- \to \bar{f}f\gamma\gamma$, production of four fermions $e^+e^- \to \bar{f}f\bar{f}'f'$ etc., if necessary.

It should be noted, however, that there exist specialized techniques [19, 20, 21] for

calculating QED spin amplitudes for almost massless fermions which, in this particular case, may be more efficient. Here I consider methods which apply to a more general case of fermions with finite masses, but a limit of small masses may be easily taken.

The methods advocated in this Section consist of eliminating from spin amplitudes, as given by Feynman rules, Dirac spinors for external fermions and strings of γ matrices at the early stage of the calculations. This is accomplished by cutting off the amplitude of pairs of external spinors by means of the Fierz identity. The external parts are calculated in the rest frames of the fermion pairs and the rest of expression includes rather short γ traces, easily calculable[2]. The resulting expressions consists of components which are tensors with only Lorentz vector indices. The individual component tensors are calculated in convenient reference frames and the appropriate Lorentz transformations are then applied, before the contractions are affected.

The resulting, Lorentz invariant spin amplitudes are expressed in terms of the same independent variables, angles and velocities, which were used to parametrize spin states, momenta and the phase space.

First, I shall introduce a notation with a simple example of the lowest order spin amplitudes. Then, I shall demonstrate more involved calculations of spin amplitudes with examples of the box diagrams and hard bremsstrahlung.

Lowest order

The lowest order, one photon exchange, amplitude for the process $e^+(p_1)+e^-(p_2) \to \tau^+(q_1)+\tau^-(q_2)$, as obtained from Feynman rules [22], reads:

$$M^0 = ie^2qq'(p_1+p_2)^{-2}\bar{v}(e^+)\gamma^\mu u(e^-)\bar{u}(\tau^-)\gamma_\mu v(\tau^+), \tag{3.1}$$

where eq and eq' are the charges of e^+ and τ^+. If, for the external fermions, the wave functions $|e^\pm; p_i, \lambda_i\rangle$ and $|\tau^\pm; q_i, \alpha_i\rangle$ defined in Section 3 are being used, then the following spinors enter in (3.1)

$$\begin{aligned} v(e^+; p_1, \lambda_1) &= S(L_0(e^+))v(\mathring{p}, \lambda_1), \\ u(e^-; p_2, \lambda_2) &= S(L_0(e^-))u(\mathring{p}, \lambda_2), \\ v(\tau^+; q_1, \alpha_1) &= S(L_0(\tau^+))v(\mathring{q}, \alpha_1), \\ u(\tau^-; q_2, \alpha_2) &= S(L_0(\tau^-))u(\mathring{q}, \alpha_2), \end{aligned} \tag{3.2}$$

where $S(L)$ represents Lorentz transformation L, see Ref. [22] for its explicit definition. Spinor $u(\mathring{p}, \lambda)$ ($v(\mathring{p}, \lambda)$) represents a fermion (antifermion) in its rest frame, $\mathring{p} = (m, 0, 0, 0)$, with spin projection λ on the third axis. These spinors, with γ matrices defined as in Ref. [22], are the following:

$$\begin{aligned} u(\mathring{p}, \alpha) &= \begin{pmatrix} \varphi_\alpha \\ 0 \end{pmatrix}, \quad v(\mathring{p}, \alpha) = C\bar{u}(\mathring{p}, \alpha) = \begin{pmatrix} 0 \\ \chi_\alpha \end{pmatrix}, \\ \varphi_{1/2} &= \begin{pmatrix} 1 \\ 0 \end{pmatrix}, \quad \varphi_{-1/2} = \begin{pmatrix} 0 \\ 1 \end{pmatrix}, \quad \chi_\alpha = i\sigma_2\varphi_\alpha. \end{aligned} \tag{3.3}$$

[2] The author acknowledges helpful discussion with dr. R. Kleiss on this point.

Putting all this together one obtains for lowest order spin amplitudes

$$\mathcal{M}^0_{\lambda_1\lambda_2\alpha_1\alpha_2} = ie^2qq'(p_1+p_2)^{-2}V^\mu_{\lambda_1\lambda_2}\tilde{V}_{\mu,\alpha_1\alpha_2}, \tag{3.4}$$

where

$$V^\mu_{\lambda_1\lambda_2} = R_3(\varphi)^\mu{}_\nu \bar{v}(\mathring{p},\lambda_1)\bar{S}(B_3(\eta_e))\gamma^\nu S(B_3(-\eta_e))u(\mathring{p},\lambda_2),$$

$$\tilde{V}^\mu_{\alpha_1\alpha_2} = [R_3(\varphi)R_1(-\theta)]^\mu{}_\nu \bar{u}(\mathring{q},\alpha_2)\bar{S}(B_3(-\eta_\tau))\gamma^\nu S(B_3(\eta_\tau))v(\mathring{q},\alpha_1),$$

and $\bar{S} = \gamma^0 S^+ \gamma^0$. Note that V and $\tilde{V}$ are defined here in CMS. The standard transformation properties of spinors were used to isolate the rotation outside V and $\tilde{V}$. The rotation $R_3(\varphi)$ cancels, however, out in the product $V_\mu \tilde{V}^\mu$, and the resulting spin amplitudes

$$\mathcal{M}^0_{\lambda_1\lambda_2\alpha_1\alpha_2} = -ie^2qq'(p_1+p_2)^{-2}\underline{V}^\mu_{\lambda_1\lambda_2}(\eta_e)R(-\theta)_{\mu\nu}\underline{V}^\nu_{\alpha_1\alpha_2}(\eta_\tau) \tag{3.5}$$

do not depend on φ but only on θ.

The vertices $\underline{V}$ and $\underline{\tilde{V}}$ are defined in the rest frame of the corresponding fermion pair, i.e. in CMS_1 and QMS, where fermion momenta are opposite to each other and parallel to the third axis. They are easily calculable taking spinors (3.3) and the boost transformation $S(B_3(\eta)) = \exp(\frac{1}{2}\gamma_0\gamma_1\eta)$. I shall list, however, for the purpose of other applications later in this Section, not only them but all possible Fierz vertices defined as

$$F_J(\eta)_{\alpha\beta} = \bar{v}(\mathring{p},\alpha)S(B_3(\eta))\Gamma_J S(B_3(-\eta))u(\mathring{p},\beta), \tag{3.6}$$

where

$$\Gamma_J = I, \gamma_5, \gamma^\mu, \gamma_5\gamma^\mu, [\gamma^\mu,\gamma^\nu], \quad \text{for} \quad J = \mathrm{S, P, V, A, T.}$$

The analogous vertices

$$\tilde{F}_J(\eta)_{\alpha\beta} = \bar{u}(\mathring{q},\beta)S(B_3(-\eta))\Gamma_J S(B_3(\eta))v(\mathring{q},\alpha) \tag{3.7}$$

are related to the former ones as follows

$$\tilde{F}_J(\eta)_{\alpha\beta} = \pm(F_J(\eta)_{\alpha\beta})^*, \tag{3.8}$$

where a minus sign should be taken for $J = \mathrm{P, T}$.

All Fierz vertices, and later also spin amplitudes, are spanned on four simple real tensors

$$b^1_{\alpha\beta} = 2\alpha\delta_{\alpha\beta}, \quad b^2_{\alpha\beta} = \delta_{\alpha\beta}, \quad b^3_{\alpha\beta} = 2\alpha\delta_{\alpha,-\beta}, \quad b^4_{\alpha\beta} = \delta_{\alpha,-\beta},$$

and omitting indices α, β they read:

$$F_\mathrm{S} = -\sinh\eta b^4, \quad F_\mathrm{P} = -\cosh\eta b^3,$$

$$F^\mu_\mathrm{V} = \cosh\eta(b^1\delta^\mu_1 + ib^2\delta^\mu_2) - b^4\delta^\mu_3,$$

$$F^\mu_\mathrm{A} = \sinh\eta(b^2\delta^\mu_1 + ib^1\delta^\mu_2) - b^3\delta^\mu_0,$$

$$\tfrac{1}{2}F^{\mu\nu}_\mathrm{T} = -b^1\varepsilon^{\mu\nu}_{01} - ib^2\varepsilon^{\mu\nu}_{02} + \cosh\eta b^4\varepsilon^{\mu\nu}_{03} - i\sinh\eta b^3\delta^{\mu\nu}_{12}, \tag{3.9}$$

$$\text{where } \varepsilon^{\mu\nu}_{\varrho\sigma} = \delta^\mu_\varrho\delta^\nu_\sigma - \delta^\mu_\sigma\delta^\nu_\varrho.$$

Substituting $\underset{\sim}{V}^\mu = F_V^\mu$ and $\underset{\sim}{\tilde{V}}^\mu = F_V^\mu$ into Eq. (3.5), and $m_e = 0$ wherever possible, one obtains:

$$\mathcal{M}^0_{\lambda_1\lambda_2\alpha_1\alpha_2} = \mathcal{N}(b^1_{\lambda_1\lambda_2}b^1_{\alpha_1\alpha_2} + \cos\theta b^2_{\lambda_1\lambda_2}b^2_{\alpha_1\alpha_2}$$

$$+ iM\sin\theta b^2_{\lambda_1\lambda_2}b^4_{\alpha_1\alpha_2}) = \mathcal{N}\sum_{i,j=1}^{4} T_{ij}b^i_{\lambda_1\lambda_2}b^j_{\alpha_1\alpha_2}, \tag{3.10}$$

where $\mathcal{N} = -ie^2qq'(p_1+p_2)^- \cosh\eta_e \cosh\eta_\tau$.

The components of tensor T_{ij} are (also in the hard bremsstrahlung case) usually given by algebraic expressions about four times shorter than the original $\mathcal{M}$-amplitudes. In this, lowest order, case its only three nonzero components are

$$T^0_{11} = 1, \quad T^0_{22} = \cos\theta, \quad T^0_{24} = iM\sin\theta. \tag{3.11}$$

Virtual corrections

Most of the $O(\alpha^2)$ virtual corrections to the lowest order spin amplitudes (3.11) are in a sense trivial, because their amplitudes, as obtained from Feynman rules, are directly expressible in terms of the Fierz vertices F_J and $\tilde{F}_J$ (as in the lowest order). I omit them from discussion referring the reader to Refs [10] and [11], except for the interesting case of the box diagrams[3].

Let us take one of them i.e. a box with two uncrossed photons in a loop. Its amplitude reads:

$$\mathcal{M}^a = (e^2qq')^2(2\pi)^{-4}\int_k \bar{v}(e^+)\gamma^\mu(\not{k}_1+m)\gamma^\nu u(e^-)$$

$$\times\bar{u}(\tau^-)\gamma_\nu(\not{k}_2+M)\gamma_\mu v(\tau^+), \tag{3.12}$$

where

$$\int_k f(k) = \int d^4k f(k)\,[(k_1^2-m^2)(k_2^2-M^2)(k+p)^2(k-p)^2]^{-1},$$

$$k_1 = k - \frac{p_1-p_2}{2}, \quad k_2 = k - \frac{q_1-q_2}{2}, \quad p = \frac{p_1+p_2}{2}.$$

Here, in order to isolate the external spinors and to get rid of γ^μ matrices, I have to use twice the Fierz identity

$$\delta_{\alpha\beta}\delta_{\gamma\delta} = \tfrac{1}{4}\sum_J \Gamma^J_{\alpha\delta}\Gamma_{J,\gamma\beta}, \tag{3.13}$$

where the matrices Γ^J, $J = S, P, V, A, T$ are equal to Γ_J except for two: $\Gamma^T = -\Gamma_T/8$ and $\Gamma^A = -\Gamma_A$. The contractions over all vector indices are understood implicitly, for instance

$$\Gamma^T_{\alpha\beta}\Gamma_{T,\gamma\delta} = -\tfrac{1}{8}[\gamma^\mu,\gamma^\nu]_{\alpha\delta}[\gamma_\mu,\gamma_\nu]_{\gamma\beta}.$$

The result is

$$\mathcal{M}^a_{\lambda_1\lambda_2\alpha_1\alpha_2} = \sum_{I,J}\bar{v}(e^+;p_1,\lambda_1)\Gamma_I u(e^-;p_2,\lambda_2)K^{IJ}$$

$$\times\bar{u}(\tau^-;q_2,\alpha_2)\Gamma_J v(\tau^+;q_1,\alpha_1), \tag{3.14}$$

[3] Another virtual contribution with nontrivial spin structure comes from the magnetic part of vertex correction [10].

where

$$K^{IJ} = \tfrac{1}{16}(e^2qq')^2(2\pi)^{-4}\int_k \mathrm{Tr}\,(\Gamma^I\gamma^\mu(\not{k}_1+m)\gamma^\nu)\,\mathrm{Tr}\,(\gamma_\nu(\not{k}_2+M)\gamma_\mu\Gamma^J).$$

The kernel K^{IJ} may be calculated using standard trace theorems, see Ref. [10] for more details. Let us note only that in this shorthand notation it contains up to four vector indices (in K^{TT}).

Proceeding, then, in the same way as in the case of the lowest order I find

$$\mathscr{M}^a_{\lambda_1\lambda_2\alpha_1\alpha_2} = \sum_{I,J} F_I(\eta_e)_{\lambda_1\lambda_2}K^{IJ}[R_1(-\theta)\tilde{F}_J](\eta_\tau)_{\alpha_1\alpha_2}, \tag{3.15}$$

where F_I and $\tilde{F}_J$ are listed in (3.9) and the rotation $R_1(-\theta)$ acts on all vector indices in $\tilde{F}_J$.

The rest of the calculations and the resulting tensor T_{ij} for two box diagrams may be found in Ref. [10]. Here I only want to point out that the above calculation algorithm is quite general, and it applies to all virtual corrections and to hard bremsstrahlung as well, leading to a decomposition

$$\mathscr{M} \sim \sum_{I_1\cdots I_n} K_{I_1\cdots I_n}F^{I_1}\cdots F^{I_n}, \tag{3.16}$$

where every $F^{I_i}_{\alpha\beta}$ corresponds to an open fermion line in the Feynman diagram.

Hard bremsstrahlung

The calculations of spin amplitudes for the process $e^+e^- \to \tau^+\tau^-\gamma$ are, on one hand, less complicated than for box diagrams, because the Fierz identity has to be used only once, i.e. for the fermion line to which the radiative photon is attached. However complications arise, as compared to the nonradiative case, from more complex kinematics.

From Feynman rules the bremsstrahlung scattering spin amplitudes read:

$$\mathscr{M}_{\lambda_1\lambda_2\alpha_1\alpha_2\beta} = ie^2qq'\left\{\frac{eq}{(q_1+q_2)^2}H^\mu_{\lambda_1\lambda_2\beta}\tilde{V}_{\mu\alpha_1\alpha_2} + \frac{eq'}{(p_1+p_2)^2}V_{\mu\lambda_1\lambda_2}\tilde{H}^\mu_{\alpha_1\alpha_2\beta}\right\} \tag{3.17}$$

$$V^\mu_{\lambda_1\lambda_2} = \bar{v}(e^+;p_1,\lambda_1)\gamma^\mu u(e^-;p_2,\lambda_2),$$

$$\tilde{V}^\mu_{\alpha_1\alpha_2} = \bar{u}(\tau^-;q_2,\alpha_2)\gamma^\mu v(\tau^+;q_1,\alpha_1),$$

$$H^\mu_{\lambda_1\lambda_2\beta} = \bar{v}(e^+;p_1,\lambda_1)\left[-(2k\cdot p_1)^{-1}\not{\varepsilon}_\beta(-\not{p}_1+\not{k}+m)\gamma^\mu\right.$$

$$\left.-(2k\cdot p_2)^{-1}\gamma^\mu(\not{p}_2-\not{k}+m)\not{\varepsilon}_\beta\right]\bar{u}(e^-;p_2,\lambda_2),$$

$$\tilde{H}^\mu_{\alpha_1\alpha_2\beta} = \bar{u}(\tau^-;q_2,\alpha_2)\left[(2k\cdot q_1)^{-1}\gamma^\mu(-\not{q}_1-\not{k}+M)\not{\varepsilon}_\beta\right.$$

$$\left.+(2k\cdot q_2)^{-1}\not{\varepsilon}_\beta(\not{q}_2+\not{k}+M)\gamma^\mu\right]v(\tau^+;q_1,\alpha_1).$$

Note that the two terms proportional to eq and eq' represent bremsstrahlung from the initial and final state.

Let us concentrate on the calculations of spin amplitudes for the hard bremsstrahlung

from the final state $\tau^{\pm}$ fermions. In that case one finds that the QMS_γ reference system is quite convenient for calculations, although any of the systems between CMS_1 and QMS in Fig. 1b might also be used.

The Fierz vertex $V^{\mu}_{\lambda_1\lambda_2}$ for an $e^{\pm}$ pair may be taken from Eqs (3.9) in CMS_1 and transformed to QMS_γ

$$V^{\mu}_{\lambda_1\lambda_2} = [R_3(-\varphi_2)B_3(\zeta)R_1(\theta_1)]^{\mu}{}_{\nu}F^{\nu}_{V}(\eta_e)_{\lambda_1\lambda_2}. \tag{3.18}$$

The calculations of $\tilde{H}^{\mu}$ in QMS_γ proceed as follows. First, the Fierz identity is applied in order to isolate $\tau^{\pm}$ external spinors

$$\tilde{H}^{\mu}_{\alpha_1\alpha_2\beta} = \tfrac{1}{4}\sum_J \mathrm{Tr}\,\{[(2k\cdot q_1)^{-1}\gamma^{\mu}(-\not{q}_1 - \not{k}_1 + M)\not{\varepsilon}_\beta$$

$$+(2k\cdot q_2)^{-1}\not{\varepsilon}_\beta(\not{q}_2 + \not{k} + M)\gamma^{\mu}]\Gamma^J\}\bar{u}(\tau^-; q_2, \alpha_2)\Gamma_J v(\tau^+; q_1, \alpha_1). \tag{3.19}$$

The trace with up to five γ^{μ} matrices is expressed in terms of vectors $k, q_1, q_2, \varepsilon_\beta$. The $\tau^{\pm}$ Fierz vertices are taken from (3.9) in QMS and transformed to QMS_γ

$$\bar{u}(\tau^-; q_2, \alpha_2)\Gamma_J v(\tau^+; q_1, \alpha_1) = R_1(-\theta_2)\tilde{F}_J(\eta_e)_{\alpha_1\alpha_2}.$$

As usual, $R_1(-\theta_2)$ acts on all implicit vector indices in F_J.

QMS_γ is rather convenient for evaluating all tensor algebra in Eq. (3.19), because in this system $\vec{k}$ is parallel to the third axis, $\vec{q}_1$ and $\vec{q}_2$ are anticollinear and placed in the y–z plane. Furthermore, photon polarization vectors are given simply by $\varepsilon'^{\mu}_{(\beta)} = \delta^{\mu}_{\beta}$. The resulting tensor $\tilde{H}$ in this frame is given by

$$\begin{aligned}
\tilde{H}^{\mu}_1 &= M^{-1}(1+s_\tau^2 s_2^2)^{-1}\{-b^1 s_\tau c_\tau s_2\delta^{\mu}_2 + ib^2 s_\tau c_\tau s_2 c_2\delta^{\mu}_1 \\
&\qquad + ib^3 c_\tau\delta^{\mu}_2 + b^4 s_\tau c_2^2\delta^{\mu}_1\}, \\
\tilde{H}^{\mu}_2 &= M^{-1}(1+s_\tau^2 s_2^2)^{-1}s_\zeta^{-1}\{b^1 c_\zeta s_\tau c_\tau s_2\delta^{\mu}_1 + ib^2 s_\tau c_\tau[-c_\zeta s_2 c_2\delta^{\mu}_2 + s_2^2(c_\zeta\delta^{\mu}_3 + s_\zeta\delta^{\mu}_0)] \\
&\qquad - ib^3 s_\zeta c_\tau\delta^{\mu}_1 + b^4 s_\tau[(s_\zeta - c_\zeta s_2^2)\delta^{\mu}_2 - s_2 c_2(c_\zeta\delta^{\mu}_3 + s_\zeta\delta^{\mu}_0)],
\end{aligned} \tag{3.20}$$

where indices $\lambda_1\lambda_2$ in $\tilde{H}_{\lambda_1\lambda_2\beta}$ and $b^k_{\lambda_1\lambda_2}$ were omitted, $s_\zeta = \sinh\zeta$, $c_\zeta = \cosh\zeta$, $s_\tau = \sinh\eta_\tau$, $c_\tau = \cosh\eta_\tau$, $s_i = \sin\theta_i$ and $c_i = \cos\theta_i$.

Finally, the spin amplitudes for final state bremsstrahlung are obtained by contracting V^{μ} from Eq. (3.18) with $\tilde{H}_{\mu}$ from (3.20) in QMS_γ. The result is conveniently parametrized by coefficients T^{β}_{ij} in the decomposition [11]

$$\mathscr{M}_{\lambda_1\lambda_2\alpha_1\alpha_2\beta} = \mathscr{N}\sum_{i,k=1}^{4} T^{\beta}_{ik}b^i_{\lambda_1\lambda_2}b^k_{\alpha_1\alpha_2}. \tag{3.21}$$

The calculation of the spin amplitudes for the initial state bremsstrahlung is quite analogous, and it is most conveniently done in CMS_γ. The combined result for both types of bremsstrahlung in terms of tensor T^{β}_{ik} reads

$$T^{\beta}_{ik} = (c_\zeta + s_\zeta)s_\zeta^{-1}(m^2 + s_1^2)^{-1}qt^{\beta}_{ik} + s_\zeta^{-1}c_\tau^2(1+s_\tau^2 s_2^2)^{-1}q't'^{\beta}_{ik}, \tag{3.22}$$

where the two complex tensors t and t' are relatively simple and their components are listed in Ref. [11].

4. *Individually adapted Monte Carlo algorithms: Summa technologiae*

In this Section I review the elementary methods of constructing efficient Monte Carlo algorithms individually adapted to a given multidimensional distribution (IAMC methods). As was pointed out, such methods are of great interest for M.C. integration over the multi-body phase space in many QED/STPI processes. Here, I shall discuss them in general terms, not specifying a distribution to be generated. The discussion will be restricted to the methods which provide, as a final result, events with constant weights (direct M.C. simulation).

It is known that the most efficient M.C. algorithms are those which are individually adapted to a generated distribution and are based on the detailed knowledge of its properties. The general purpose programs [23, 24] which do not require such knowledge and adjust automatically a generation procedure to properties of the distribution are rather time-wasteful in comparison with IAMC algorithms, especially for distributions with strong and complicated peaks (the QED case). They may be useful, however, in solving quickly some problems by brute force. On the other hand, IAMC algorithms, although efficient, are rather laborious in preparation and tests.

It seems, at the first instance, that there are no systematic ways of constructing IAMC algorithms, and the invention of such algorithm is only a matter of art and experience. One learns, however, from inspection of a series of such algorithms, that they are built up using a rather limited set of basic methods in a recursive way. These elementary methods may be grouped as follows; analytical partial integration (API), rejection technique (RT), branching method (BRM), and the change of the variables (CHV).

In this Section I shall describe the above basic methods, and I shall also address the question of how one should assemble them into an efficient IAMC algorithm.

Analytical integration

The first of the elementary methods, analytical partial integration (API), may allow the problem of generating a positive, integrable, n-dimensional, unnormalized distribution $\varrho(\alpha_1 \dots \alpha_a; x_1 \dots x_n)$ to be divided into a series of less-dimensional generation problems. Variables $\alpha_1 \dots \alpha_a$ are constant parameters in the problem, but if the generation of ϱ is a part of some larger M.C. algorithm, then they may include the variables of this external M.C. problem (which have been already randomly generated).

If one is able to integrate analytically over a subset of x-variables $x_{k+1} \dots x_n$, $k < n$, or the result of integration is known from some symmetry principle, then the variables $x_1 \dots x_n$ may be generated in two steps; first, $x_1 \dots x_k$ are generated according to a partially integrated distribution

$$\varrho^{(1)}(\alpha_1 \dots \alpha_a; x_1 \dots x_k) = \int dx_{k+1} \dots dx_n \varrho(\alpha_1 \dots \alpha_a; x_1 \dots x_n), \tag{4.1}$$

and afterwards $x_{k+1} \dots x_n$ are generated according to the original distribution

$$\varrho^{(2)}(\alpha_1 \dots \alpha_a, x_1 \dots x_k; x_{k+1} \dots x_n) = \varrho(\alpha_1 \dots \alpha_a; x_1 \dots x_n), \tag{4.2}$$

where $x_1 \dots x_k$ are now treated as constants, along with $\alpha_1 \dots \alpha_a$. This method has a simple graphical representation as a split along the generation chain, see Fig. 2a.

Example 1. Let us take as an example the distribution

$$\varrho(\alpha; x_1, x_2) = (1-x_1-x_2)^{\alpha}\theta(1-x_1-x_2), \quad 0 \leqslant x_i \leqslant 1. \tag{4.3}$$

In this case

$$\varrho^{(1)}(\alpha; x_1) = (1+\alpha)^{-1}(1-x_1)^{1+\alpha}\theta(1-x_1),$$
$$\varrho^{(2)}(\alpha, x_1; x_2) = (1-x_1-x_2)^{\alpha}\theta(1-x_1-x_2). \tag{4.4}$$

For certain distributions this procedure may be repeated $n-1$ times ultimately reducing the original n-dimensional problem to a series of 1-dimensional problems, see Fig. 3a, with the following subdistributions:

$$\varrho^{(1)}(\alpha; x_1) = \int dx_2 \dots dx_n \varrho(\alpha; x),$$
$$\varrho^{(2)}(\alpha, x_1; x_2) = \int dx_3 \dots dx_n \varrho(\alpha; x),$$
$$\dots\dots\dots\dots\dots\dots\dots\dots\dots\dots$$
$$\varrho^{(n-1)}(\alpha, x_1 \dots x_{n-2}; x_{n-1}) = \int dx_n \varrho(\alpha; x),$$
$$\varrho^{(n)}(\alpha, x_1 \dots x_{n-1}; x_n) = \varrho(\alpha; x), \tag{4.5}$$

where $\varrho(\alpha; x)$ stands for $\varrho(\alpha_1 \dots \alpha_a; x_1 \dots x_n)$. In this way the problem is solved almost to the end because, as will be shown later in this Section, there exist many methods of generating 1-dimensional distributions. The example 1 also demonstrates such a situation.

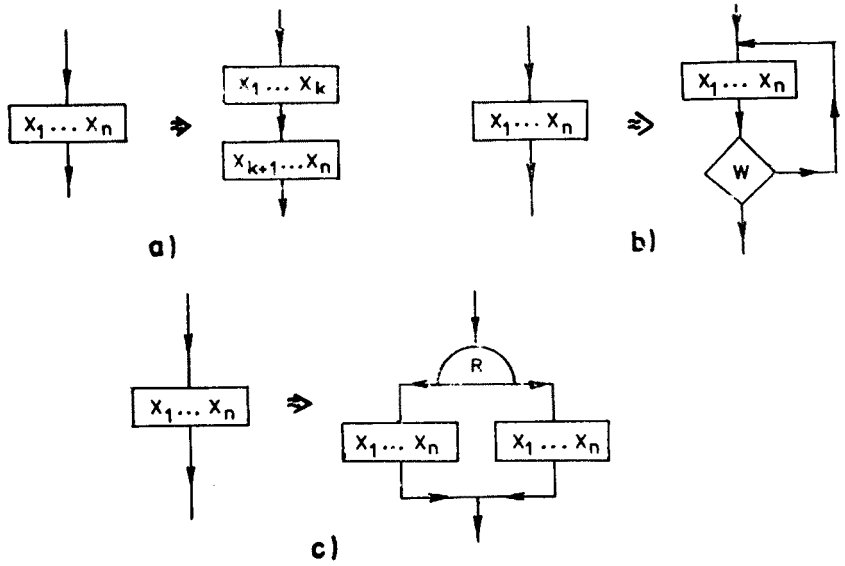

Fig. 2. Graphic representations for three basic IAMC methods: a) analytical partial integration API, b) rejection technique RT, c) branching method BRM

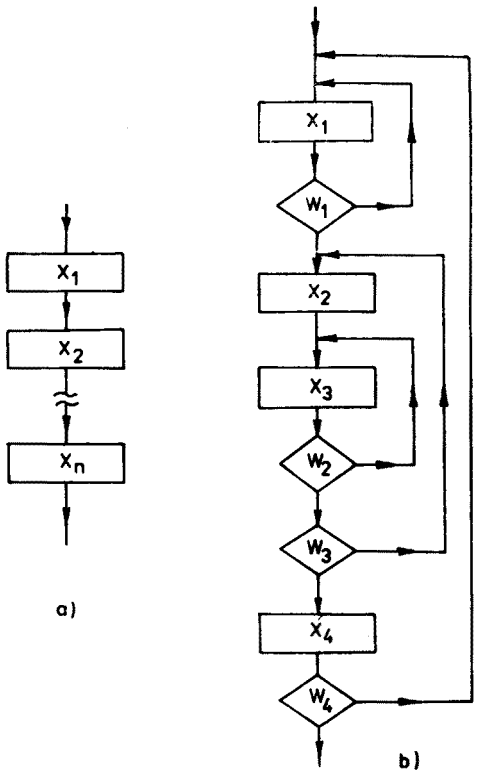

Fig. 3. The examples of the multiple (recursive) use of: a) API method, b) API and RT methods

Quite often, however, the use of the API method for any subset of x-variables is either impossible or very difficult. In this case the second of the elementary methods (RT) may be employed in order to replace the distribution $\varrho(\alpha; x)$ by a simpler one, before a new attempt of the use of API is made.

Rejection technique

For this second method to be used one has to find a distribution $\varrho_D(\alpha_1 \ldots \alpha_a; x_1 \ldots x_n)$ which is as close to $\varrho(\alpha; x)$ as possible, but simpler than $\varrho(\alpha; x)$, and obeying an inequality $\varrho_D \geqslant \varrho$. I shall refer to ϱ_D as a dominant distribution (DD) with respect to ϱ.

The method consists in generating raw points $x_1 \ldots x_n$ according to distribution ϱ_D (simpler than ϱ) and then in rejecting some of the raw events in such way that as a result the accepted events are distributed according to ϱ.

More precisely the weight

$$w = \varrho/\varrho_D \tag{4.6}$$

is compared with the uniform random number $r \in (0, 1)$ for every raw event and the event is accepted if $r \leqslant w$, otherwise it is rejected.

The efficiency of the method, i.e. the rate of the accepted events

$$e = N_{\text{accepted}}/(N_{\text{accepted}}+N_{\text{rejected}}), \tag{4.7}$$

which measures the closeness of the functions ϱ and ϱ_D is also equal to the ratio of the corresponding integrals

$$e = \int \varrho(\alpha; x)d^n x/\int \varrho_D(\alpha; x)d^n x = \langle w\rangle, \tag{4.8}$$

and to the average weight $\langle w\rangle$, calculated using the total sample of the raw points. Ideally this efficiency should be as close to unity as possible, but in practice $e \gtrsim 1/10$ is acceptable. For smaller e one should look for a better ϱ_D.

Eq. (4.8) is also often used to calculate numerically the integral $\int \varrho d^n x$ from $e = \langle w\rangle$ ($\langle w\rangle$ calculated from a finite M. C. sample), provided that the simpler integral $\int \varrho_D(\alpha; x)d^n x$ is known.

At this moment, a natural question to be asked is whether there is any systematical way of finding the ϱ_D distribution. The simple answer is that one has to guess it. In the case of a mild variation of ϱ (logarithmic, polynomial etc.), simply a constant equal to the maximum value of ϱ can be used as ϱ_D. This choice will lead, however, to excessive rejection for strongly peaked distributions ϱ. Quite often, a good hint on ϱ_D may be learned from inspection of some approximate, even crude, method of calculating (or merely estimating) the integral

$$\sigma(\alpha) = \int \varrho(\alpha; x)d^n x. \tag{4.9}$$

Usually such a method is founded on some approximation (simplification) made on ϱ. This approximation, or sometimes its modification assuring $\varrho_D \geqslant \varrho$, may be used as a good candidate for ϱ_D in RT.

The new distribution ϱ_D effectively replaces the original distribution ϱ in the generation problem. Hopefully, if ϱ_D is simple enough, the API method may be used successfully, replacing the generation of ϱ_D with a chain of less-dimensional subgenerations. Then, in turn, the RT may be applied again, to simplify the subdistributions resulting from API, and so on.

The art of constructing an efficient IAMC algorithm consists in a skilful alternate use of the two above methods (API, RT) until one is left with only a chain of 1-dimensional subgenerations. This recursive use of the API and RT leads to an algorithm which in a graphical representation has a single generation chain with nested rejection loops, as in an example in Fig. 3b.

The RT may be used, in particular, to simplify the 1-dimensional distribution before some other method for its generation is used.

Example 2. For distribution (4.3) with $0 < \alpha \lesssim 3$ the simplest possible ϱ_D is

$$\varrho_D(\alpha; x_1, x_2) = \theta(1-x_1)\theta(1-x_2). \tag{4.10}$$

In this case $w = \varrho$ and the x_1, x_2 of a raw point are generated independently in the (0, 1) range.

Branching method

It may easily happen that the generation problem cannot be solved with the two elementary methods (API, RT) described so far. In this case, the third method, leading to a branching of the algorithm into two or more parallel generation chains (BRM) may appear to be helpful.

It applies when the distribution $\varrho(\alpha; x)$ in question can be split in a natural way into a sum of two (or more) positive subcomponents

$$\varrho(\alpha; x) = \varrho^{(1)}(\alpha; x) + \varrho^{(2)}(\alpha; x). \tag{4.11}$$

Without any loss of generality, I allow here the already generated (up to a branching point) x-variables to be hidden among constants $\alpha_1 \ldots \alpha_a$.

At the branching point the ratio

$$R(\alpha) = \sigma^{(1)}(\alpha)/(\sigma^{(1)}(\alpha) + \sigma^{(2)}(\alpha)),$$
$$\sigma^{(i)}(\alpha) = \int \varrho^{(i)}(\alpha; x) d^n x, \tag{4.12}$$

is compared with the uniform random number $r \in (0, 1)$. If $r < R$ then x-point is generated according to $\varrho^{(1)}$, otherwise ($r \geqslant R$) according to $\varrho^{(2)}$, see also Fig. 3c for a pictorial representation for BRM. A generalization to 3 or more branches is straightforward.

BRM is also quite often used for 1-dimensional distributions, for example in the simple case of the distribution $\varrho(\alpha, \beta; x) = x^\alpha + x^\beta$, $x \in (0, 1)$, x-points are most easily generated separately for x^α and x^β components.

A particular example of BRM is the symmetrization procedure. If $\varrho(\alpha; x)$ is a sum of terms which are obtained one from another by a certain symmetry transformation, then the generation may be done using only one of such components and afterwards a random symmetrization with the adequate probabilities, is performed.

In certain cases, the generation procedure has to be constructed in a different way in two (or more) separate subdomains $\Omega^{(1)}$ and $\Omega^{(2)}$ of the integration domain $\Omega = \Omega^{(1)} \bigcup \Omega^{(2)}$. This can also be treated using BRM with

$$\varrho^{(1)}(\alpha; x) = \theta(x)\varrho(\alpha; x),$$
$$\varrho^{(2)}(\alpha; x) = (1 - \theta(x))\varrho(\alpha; x), \tag{4.13}$$

where $\theta(x) = 1$ for $x \in \Omega^{(1)}$ and $\theta(x) = 0$ for $x \notin \Omega^{(1)}$.

The very important property of BRM is that the generation in every branch is totally independent, and in every branch one may separately use the API and RT exploring further properties of the component distributions $\varrho^{(i)}(\alpha; x)$.

In a graphical representation, the IAMC algorithm exploiting API, RT and BRM may have rejection loops on the branches and the branched subgenerations nested in some larger rejection loops. This structure may be seen in one of the examples discussed in the next Section (see Fig. 7).

The change of the integration variables (mapping)

The rôle of a good choice of the integration variables cannot be underestimated. In API this often solves the problem of the partial analytical integration.

In RT the appropriate choice of variables may reveal the structure of the most important singularities (peaks) in ϱ, allowing a simple ϱ_D possessing the same singularities as ϱ to be found.

The real power of BRM unfolds, when it is combined with the change of variables (CHV). This comes from the fact that one may use in every i-th branch a different set of integration variables $x_1^{(i)} \dots x_n^{(i)}$ adapting their choice to properties of $\varrho^{(i)}(\alpha; x)$.

The change of variables $x(y)$ introduces the Jacobian factor in $\varrho(\alpha; x)$,

$$\varrho(\alpha; x)d^n x = |\partial x/\partial y|\varrho(\alpha; x(y))d^n y = \varrho'(\alpha; y)d^n y. \tag{4.14}$$

In principle one could even solve entirely the problem of generating ϱ by finding such $x(y)$ that $|\partial x/\partial y| = \varrho^{-1}$, i.e. $\varrho'(\alpha; y) \equiv 1$.

Although, in a multidimensional case, finding such $x(y)$ (in analytical form) is usually impossible, the above method is applied often in the 1-dimensional case. For such distributions $\varrho(\alpha; x)$, $x \in (a, b)$, one has to invert the cumulative function

$$F(\alpha; x) = \int_a^x \varrho(\alpha; x')dx' / \int_a^b \varrho(\alpha; x')dx', \tag{4.15}$$

with respect to x and $x = x(y) = F^{-1}(y)$, $y \in (0, 1)$, is distributed according to $\varrho(\alpha; x)$ provided that y is generated uniformly.

Unfortunately only for a limited number of simple distributions like x^α, $e^{\alpha x}$, $\sin x$, $(1-x^2)^{-1}$ etc, which are derivatives of the elementary functions, the cumulative functions may be inverted analytically. A numerical inversion of the cumulative function is relatively easy if there exists an analytical expression for $F(\alpha; x)$.

In practice the best method of generating 1-dimensional distribution is to use RT and BRM so long as one is finally left with a set of simple 1-dimensional distributions which can be generated by an analytical inversion of their cumulative functions.

In example 1, the two subdistributions $\varrho^{(i)}$, $i = 1, 2$, may be generated by inversion of their cumulative functions

$$\begin{aligned} x_1 &= 1-\exp((\alpha+2)^{-1} \ln y_1), \\ x_2 &= (1-x_1)(1-\exp((\alpha+1)^{-1} \ln y_2), \end{aligned} \tag{4.16}$$

where $y_i \in (0, 1)$ are generated with uniform probability. If, in the n-dimensional case, the generation of ϱ may be replaced by a chain of n 1-dimensional distributions as in (4.5) (API method), then the problem of finding $x(y)$ such that $\varrho' \equiv 1$ can be solved by numerical or analytical inversion of the cumulative functions for all $\varrho^{(i)}$, $i = 1 \dots n$ in (4.5), similarly as in (4.16).

Evaluation of the integral

Quite often, one is also interested in the value of the integral

$$\sigma(\alpha) = \int \varrho(\alpha; x)d^n x. \tag{4.17}$$

It should be noted immediately that the problem of the numerical evaluation of the integral

(4.17) using the M.C. method and the problem of generating x-points according to $\varrho(\alpha; x)$ are practically equivalent.

If the M.C. algorithm is built using the elementary techniques of this Section, then a set of simple rules tells us how to calculate the value of the integral (4.17).

In the case when there is no branching in the beginning of the algorithm then

$$\sigma(\alpha) = \prod_{j=1}^{p} \langle w^{(j)} \rangle \int \varrho^{(1)}(\alpha; x_1) dx_1, \tag{4.18}$$

where $\langle w^{(j)} \rangle$ are the average weights for all $j = 1 \ldots p$ rejection loops (if there are any) surrounding the generation point of the first variable x_1 in the generation chain. For instance for the algorithm of Fig. 3b

$$\sigma(\alpha) = \langle w^{(1)} \rangle \langle w^{(4)} \rangle \int \varrho^{(1)} dx_1. \tag{4.19}$$

The value of the integral $\int \varrho^{(1)} dx_1$ is usually known in the M.C. program as a byproduct of the $\varrho^{(1)}$ generation.

In a general case, the generation chain may start with a branching. In this case Eq. (4.18) is applied in every branch, and the results should be summed up over the branches. Then, the sum should be multiplied, as in (4.18), by average weights from all rejection loops surrounding the branching point (i.e. the branched part of the algorithm).

Summary of the IAMC methods

Usually there exists a sizeable freedom in a final form of the IAMC algorithm for a given distribution. The efficiency of the corresponding program may be improved by a good choice of the integration variables and good choices of the dominant distributions ϱ_D in all rejection loops. Rejection loops surrounding large parts of the algorithm should be avoided.

An optimisation for efficiency may lead, however, to a complicated topology for the algorithm, as viewed in the corresponding graph, with many branches and loops. Preparing such a program may become laborious. Usually a reasonable compromise between the simplicity and the efficiency may be found.

Keeping these remarks in the mind, the following prescription for finding an efficient IAMC algorithm may be formulated: try to find natural integration variables (CHV) which unfold properties (peaks) of the distribution; and try to perform as many analytical integrations (API) as possible, thus reducing the generation of ϱ to a series of less-dimensional subgenerations.

If the above possibilities are exploited then try to simplify ϱ with the rejection technique (RT), $\varrho \to \varrho_D$. This applies both to the original distribution ϱ and to subdistributions resulting from API.

If any subdistribution, or ϱ itself, splits naturally into a sum of positive components, then use the branching method (BRM), especially if there exists a possibility of adapting variables (CHV) to a distribution in every branch separately.

By recursive use of these methods (API, RT, BRM, CHV) one is ultimately left with a series of 1-dimensional distributions which can be generated by inverting analytically their cumulative functions or some other simple methods [25].

This Section does not, of course, exhaust all possible M.C. methods. For some other reviews on M.C. techniques see Refs [26], [27] and [28].

5. Monte Carlo simulation of the τ production and decay process

The process $e^+e^- \to \tau^+\tau^-(\gamma)$, $\tau^\pm \to X^\pm$ at highest PETRA/PEP energies is at present a main source of the valuable information on the τ lepton properties and on the τ coupling to the Z_0 boson [5]. As compared to a similar process $e^+e^- \to \mu^+\mu^-(\gamma)$ the τ pair production process is much more complicated from the point of view of data analysis: the τ lepton is unstable and visible only through its decay products (with two neutrinos always escaping detection), furthermore the main decay modes $\tau^\pm \to e^\pm$, $\mu^\pm$, $\varrho^\pm$, $\pi^\pm$ (18%, 18%, 23%, 10%) [15] are of a similar strength and are rather different from the detection point of view. Finally the background problems are also more severe than in muon production.

The emission of the radiative photon in the τ production process is known to change the total cross section and particle distributions [29, 30] by up to 30%. That, of course, makes the τ pair data analysis again more involved. The M.C. program of Ref. [11] which simulates the process $e^+e^- \to \tau^+\tau^-(\gamma)$, $\tau^\pm \to \nu_\tau \mu^\pm(e^\pm, \mu^\pm, \varrho^\pm)$ is aimed to serve as a tool, for eliminating the influence of the trivial QED, spin and mass effects on the measurements of the interesting physical quantities like τ branching ratios, coupling constants, mass of ν_τ, etc. It takes into account: order α^3 QED radiative effects including hard bremsstrahlung from the initial and final state fermions; arbitrary $e^\pm$ spin polarizations (longitudinal and transverse); the decay of each τ in its rest frame including all spin effects (polarizations, correlations); the exchange of Z_0 bosons in the low energy approximation suitable for PETRA/PEP energies including polarizations of τ's due to Z_0 exchange.

The above program is described in a complete and detailed way in its long-write-up [11]. Here, in this Section, I shall characterize the IAMC algorithm used in [11] in terms of the elementary techniques listed in Section 4. I shall comment on the way in which spin effects are introduced pointing out some possible future generalizations and developments. The algorithm for the production part $e^+e^- \to \tau^+\tau^-(\gamma)$ will be also compared with the corresponding algorithms for $e^+e^- \to \mu^+\mu^-(\gamma)$ process in Refs [29], [31] and [32].

Spin and Monte Carlo

As was pointed out in the Introduction, a good separation of the production and decay parts in the calculations (M.C. algorithm) is a very desirable property. So far, I have derived in Section 2 a compact formula for the d.c. section of the process $e^+e^- \to \tau^+\tau^-(\gamma)$, $\tau^\pm \to X^\pm$ which may be rewritten as follows:

$$d\sigma(x, y, z) = \sum_{abcd=0}^{3} \tilde{\varepsilon}^a_{(1)} \tilde{\varepsilon}^b_{(2)} R_{abcd}(x) d\tau_{\text{prod}}(x) H^c_{(1)}(y) d\tau^{(1)}_{\text{dec}}(y) H^d_{(2)}(z) d\tau^{(2)}_{\text{dec}}(z), \qquad (5.1)$$

where $d\tau_{\text{prod}} = d\tau_2, d\tau_3$ depending on the presence of the bremsstrahlung photon and variables x, y, z denote collectively the corresponding phase space variables.

The separation of the production and decay parts in the IAMC algorithm for the above process is achieved by using a combination of RT and API methods (see Section 4). I discuss two options:

(A) The API is employed using the integral

$$\int_x H^c_{(i)}(x) = \int d\tau^{(i)}_{\text{dec}}(x) H^c_{(i)}(x) = \delta_{c0}. \tag{5.2}$$

The moments of $\tau^+\tau^-(\gamma)$ are generated first, according to a partly integrated distribution

$$d\sigma^{(1)}(x) = \int_x \int_y d\sigma = \sum_{ab} \tilde{\varepsilon}^a_{(1)} \tilde{\varepsilon}^b_{(2)} R_{ab00}(x) d\tau_{\text{prod}}(x). \tag{5.3}$$

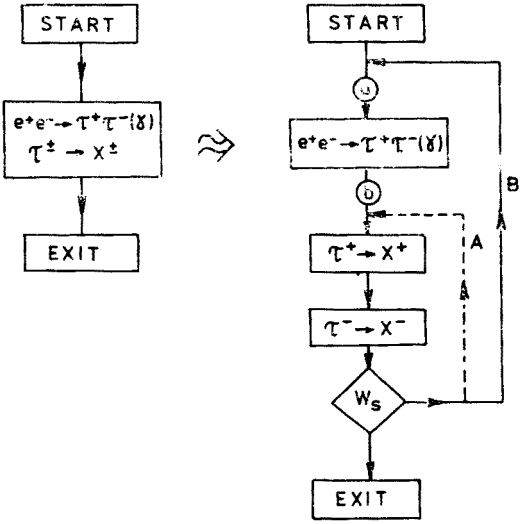

Fig. 4. Schemes of implementing spin effects in the M.C. algorithm for the τ production and decay process

In the second step, for fixed x, a double decay distribution $d\sigma^{(2)}(x; y, z) = d\sigma(x, y, z)$ is generated by means of RT with a dominant distribution and the weight being:

$$\begin{aligned} d\sigma^{(2)}_{\text{D}}(x; y, z) &= 2 \sum_{ab=0}^{3} \tilde{\varepsilon}^a_{(1)} \tilde{\varepsilon}^b_{(2)} R_{ab00}(x) \\ &\times H^0_{(1)}(y) d\tau^{(1)}_{\text{dec}}(y) H^0_{(2)}(z) d\tau^{(2)}_{\text{dec}}(z), \\ w_s = d\sigma^{(2)}/d\sigma^{(2)}_{\text{D}} &= \tfrac{1}{2} \Big(\sum_{abcd} \tilde{\varepsilon}^a_{(1)} \tilde{\varepsilon}^b_{(2)} r_{abcd} \\ &\times h^c_{(1)} h^d_{(2)} \Big) \Big(\sum_{ab} \tilde{\varepsilon}^a_{(1)} \tilde{\varepsilon}^b_{(2)} r_{ab00} \Big)^{-1}, \end{aligned} \tag{5.4}$$

where

$$r_{abcd} = R_{abcd}/R_{0000}, \qquad h^c_{(i)} = H^c_{(i)}/H^0_{(i)}.$$

This method is illustrated graphically in Fig. 4, see rejection loop marked with A.

(B) Here, RT is used first:

$$d\sigma_D(x, y, z) = 8R_{0000}(x)d\tau_{prod}(x)H^0_{(1)}(y)d\tau^{(1)}_{dec}(y)H^0_{(2)}(z)d\tau^{(2)}_{dec}(z),$$
$$w_s = d\sigma/d\sigma_D = \tfrac{1}{8}\sum_{abcd} \tilde{\varepsilon}^a_{(1)}\tilde{\varepsilon}^b_{(2)}r_{abcd}h^c_{(1)}h^d_{(2)}, \tag{5.5}$$

and then API based on Eq. (5.2). The momenta of $\tau^+\tau^-(\gamma)$ are generated according to

$$d\sigma^{(1)}_D(x) = \int_y \int_z d\sigma_D = 8R_{0000}(x)d\tau_{prod}(x). \tag{5.6}$$

This option is also depicted in Fig. 4, see rejection loop marked by B.

In both methods, see Fig. 4, the momenta of $\tau^+\tau^-(\gamma)$ are generated first, assuming polarized (A) or unpolarized (B) beams, and then the decays of $\tau^\pm$ are simulated in the $\tau^\pm$ rest frames RS($\tau^\pm$), as if the τ's were unpolarized. All spin effects in the final state (in option B also in the initial state) are introduced by the RT. Finally, the $\tau^\pm$ momenta are transformed from RS($\tau^\pm$) to CMS using transformation $L_t(\tau^\pm)$.

The rejection rate in option A is 50% precisely, and in option B varies from 0% to 100% depending on the longitudinal polarizations of $e^\pm$.

The solution B is simpler and this is the reason why it was used in Ref. [11]. The solution A, due to the fact that the production part is outside the rejection loop, is more efficient (factor $\sim$ 10) and it should be kept in mind for future developments. In fact it is also used in Ref. [11] for unpolarized $e^\pm$.

A comment on the treatment of the almost massless spin 1/2 fermions is here in order. Although, at present energies ($\sqrt{s} \leqslant 45$ GeV) the mass of the τ cannot be neglected (at 1% accuracy level), at higher energies $m_\tau \ll \sqrt{s}$ will be a good approximation. In this case, in QED and other gauge theories, spin projection may be effectively replaced by chirality, and a left/right handed τ lepton (or any other light fermion) preserves its identity in the scattering process. In this case the spin density formalism is not really necessary and spin amplitudes, or rather chirality amplitudes, may be treated in a purely probabilistic way. In the M.C. algorithm the chirality configurations may be chosen randomly [26] according to modulus-squares of the corresponding amplitudes. Also the decay of almost massless unstable fermions in flight may be taken as an incoherent superposition of the decays of the left and right handed components. All this should be done, however, in a consistent way, i.e. one should not attempt to control a relative phase of the left and right handed components. For example one should not measure directly or indirectly the transverse polarizations, for instance by measuring an azimuthal asymmetry around the beam or by measuring the transverse momenta of the decay products with respect to the momentum of the parent fermion.

Although techniques described in this work apply to a more general case of genuinely massive, possibly transversely polarized fermions, the above chiral limit may be taken, if necessary, by setting $R_{abcd} = 0$ for $a, b, c, d = 1, 2$.

Production part

The production part of the M.C. algorithm used in Ref. [11] and described briefly in the following, is to some extent similar to that of Ref. [32]: Centre of mass photon

momentum $E_\gamma = k\sqrt{s}/2$ plays a central role in both algorithms. The distribution $d\sigma/dk$ can be calculated explicitly by an analytical integration over the angular variables [30] and, therefore, the generation of k may be detached from the rest of the generation chain (API method) as shown in Fig. 5.

The d.c. section for $e^+e^- \to \tau^+\tau^-(\gamma)$ process is infrared divergent in the $E_\gamma \to 0$ region of the phase space. This region has to be isolated from the rest of the phase space and, inside, the divergent contribution from the soft bremsstrahlung is cancelled in a known way [33, 34] by the virtual contributions.

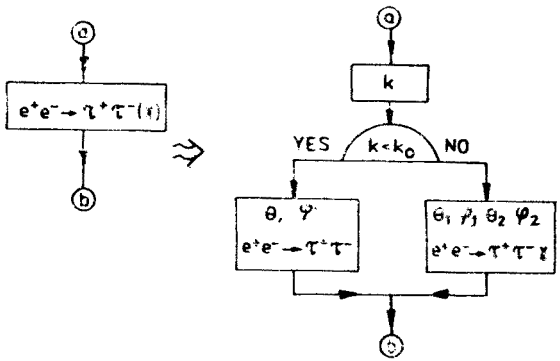

Fig. 5. The general structure of the IAMC algorithm for the τ production process

There exists a certain freedom in choosing a boundary for the infrared domain Ω_0 which may be used in the M.C. type calculations, in order to simplify the hard bremsstrahlung part of the M.C. algorithm [35] and/or to minimize the algebraic complexity of the $\sigma(\Omega_0)$ contribution from the infrared domain.

There are, however, some restrictions on the choice of Ω_0. In a real experiment any measurement of an integrated cross section, of the content of a single bin in a histogram or some asymmetry etc., is equivalent to convoluting the QED distribution with a smooth "effective acceptance" function which for any such measurement summarizes the effects due to apparatus acceptance, resolution, triggers, selection criteria, etc. It makes sense to compare the experimental result with a QED prediction, only if the result of convolution does not depend noticeably on the variation of the Ω_0 boundary i.e. the "effective acceptance" of the measurement should be constant all over Ω_0 and in its close neighbourhood. Unfortunately this cannot be achieved by simply taking Ω_0 indefinitely small, because at a given perturbative order, taking Ω_0 too small may yield a nonsense result, for example a negative cross section. Reducing Ω_0 usually costs taking the next, higher, order in the perturbative expansion.

In the M.C. calculations the positiveness of $\sigma(\Omega_0)$ is also necessary because the probability $p_0 = \sigma(\Omega_0)/\sigma_{\text{total}}$ is used in the beginning of the M.C. algorithm, see branching point in Fig. 5, to decide whether a hard photon (outside Ω_0) was emitted or not.

In Refs [11], [29] and [32], and in many other QED calculations, Ω_0 is defined by taking an upper limit on the photon CMS energy, $k < k_0$. In the energy range $2m_\tau \leqslant \sqrt{s}$

$\lesssim 45$ GeV, the "effective acceptance" of a typical measurement in an e^+e^- experiment may tolerate k_0 up to 0.05. On the other hand a positivity of $\sigma(\Omega_0(k < k_0))$ requires $k_0 \geqslant 10^{-3}$.

In the calculations for other QED processes, for example for the t-channel exchange process, it may be profitable [35] to take another choice of Ω_0.

The photon spectrum for τ production process was calculated in Ref. [30] and it has the following form

$$d\sigma/dk = (qq')^2 4\pi\alpha^2 (3s)^{-1}(\delta(k)\varrho_s + \theta(k-k_0)\varrho(k)), \tag{5.7}$$

where ϱ_s collects contributions from the lowest order, virtual contributions and soft bremsstrahlung, see graphs a–e and h–k in Fig. 6, and the function $\varrho(k)$ combines contributions

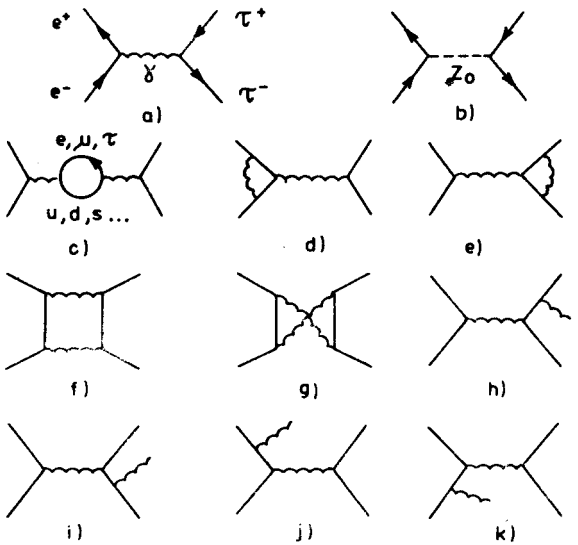

Fig. 6. Feynman diagrams of $O(\alpha^3)$ calculations for $e^+e^- \to \tau^+\tau^-$ process. Diagrams with self energy loops on the external fermion lines are omitted

from the hard bremsstrahlung, graphs h–k in Fig. 6. The explicit formulae for ϱ_s and $\varrho(k)$ may be found in Ref. [11]. In the limit $\sqrt{s} \gg m_e, m_\tau$ and $k \ll 1$ it has a familiar form [8, 36]

$$\frac{(qq')^2 4\pi\alpha^2}{3s}\left\{\left(1-2\,\mathrm{Re}\,\Pi + \frac{3\alpha q}{2\pi}\ln\frac{s}{m_e^2} + \frac{3\alpha q'}{2\pi}\ln\frac{s}{m_\tau^2}\right)\delta(k) + \left(\frac{1}{k}\right)_+ \frac{2\alpha q}{\pi}\ln\frac{s}{m_e^2} + \left(\frac{1}{k}\right)_+ \frac{2\alpha q'}{\pi}\ln\frac{s}{m_\tau^2}\right\}, \tag{5.8}$$

where $(1/k)_+ = \delta(k)\ln(k_0) + \theta(k-k_0)/k$. Now, it is explicitly seen that k_0 is merely a dummy parameter introduced to regularize the $(1/k)_+$ distribution for the M.C. purpose.

A more detailed scheme of the event generator for $e^+e^- \to \tau^+\tau^-(\gamma)$ process [11] is depicted in Fig. 7. Photon momentum k is generated first (API). Its distribution at a little cost

is simplified, $d\sigma/dk \to (d\sigma/dk)_D$, by a rejection, depicted in Fig. 7, by a loop with weight $w_k = (d\sigma/dk)/(d\sigma/dk)_D$. See Ref. [11] for a definition of $(d\sigma/dk)_D$ and a method used for its generation. After generating k the algorithm branches into soft and hard parts.

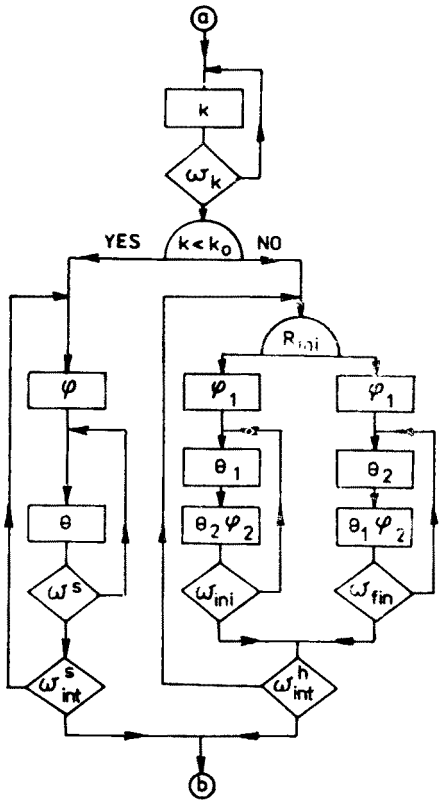

Fig. 7. The detailed scheme of the IAMC algorithm for the τ production process [11]

In the soft branch, $k < k_0$, variable $\varphi \in (0, 2\pi)$ is chosen with a uniform probability and $\cos\theta \in (-1, 1)$ distribution is obtained by a two-step rejection starting from a flat distribution. In the second rejection, with weight w^s_{int}, the contributions from graphs b, f, g in Fig. 6 are added.

In the bremsstrahlung part, $k \geqslant k_0$, the d.c. section:

$$d\sigma = (qq')\alpha^3(4\pi^2 s)^{-2}(A_{ini}+A_{fin}+A_{int})d\tau_3, \tag{5.9}$$

with A_{ini}, A_{fin}, A_{int} [10, 11] representing hard bremsstrahlung from initial electrons, final $\tau^{\pm}$ and their interference, is simplified using a rejection based on

$$d\sigma_D = (qq')\alpha^3(4\pi^2 s)^{-2}(2A_{ini}+2A_{fin})d\tau_3. \tag{5.10}$$

This is represented in Fig. 7 by a rejection loop with the weight

$$w^h_{int} = \tfrac{1}{2}(1+A_{int}/(A_{ini}+A_{fin})). \tag{5.11}$$

The generation of the raw distribution (5.10) is done separately for A_{ini} and A_{fin} (BRM). The choice of the branch is done by a comparison of the random number with

$$R_{\text{ini}} = \varrho_{\text{ini}}(k)/(\varrho_{\text{ini}}(k)+\varrho_{\text{fin}}(k)), \quad k \geqslant k_0, \tag{5.12}$$

see Fig. 7, where ϱ_{ini}, ϱ_{fin} are the contributions from A_{ini} and A_{fin} to $\varrho(k)$ (A_{int} does not contribute), see Eq. (4.12).

The above branching is done because A_{ini} and A_{fin} have peaks in different variables: A_{ini} is singular in θ_1, but mildly dependent on φ_1, φ_2 and θ_2, while A_{fin} is singular in θ_2, but weakly dependent on φ_1, φ_2 and θ_1. These properties serve as a basis for generating θ_i, φ_i by a RT in every branch.

For example $A_{\text{ini}}(k, \theta_i, \varphi_i)$ is replaced by:

$$A_{\text{ini,D}}(k, \theta_i, \varphi_i) = \text{const}\,(k)/(1-(1-m^2]\cos^2\theta_1), \tag{5.13}$$

and for raw points φ_1, φ_2 and $\cos\theta_2$ are chosen with a constant probability, while $\cos\theta_1$ is generated (using again branching and inversion of the cumulative functions) according to $A_{\text{ini,D}}$. A proper dependence on θ_i, φ_i is recovered by a rejection with the weight

$$w_{\text{ini}} = A_{\text{ini}}/A_{\text{ini,D}}. \tag{5.14}$$

The variable φ_1 is excluded from the rejection loop, see Fig. 7, because A_{ini} does not depend on φ_1 at all (API).

The generation of A_{fin} is very similar, only the roles of θ_1 and θ_2 are interchanged, see Ref. [11] for more details.

How does the above M.C. algorithm look in comparison with those of Refs [29] and [32] for $e^+e^- \to \mu^+\mu^-(\gamma)$ process? The M.C. method used in Ref. [29] is almost entirely based on API with four 1-dimensional distributions of the type (4.5), generated by numerical inversions of their cumulative functions. Branching was used only to separate hard and soft parts.

The algorithm of Ref. [32] has a similar structure to that of Fig. 7. The main difference is that, in the hard part, it has four branches instead of two and, furthermore, in every branch the kinematical variables φ_i, θ_i are defined in a different way. Although this method is elegant and finds a nice probabilistic interpretation [31, 37], a necessity of keeping four chains of kinematic variables should be regarded as a disadvantage. In addition, this method does not generalize easily to the case of heavy fermions (only at the cost of introducing even more branches).

Finally, the value of the total cross section for the production and decay process is calculated using the average weights from the M.C. generation (summarized in Figs 4 and 7) as follows

$$\text{A: } \sigma = \langle w_k \rangle \int_0^1 \left(\frac{d\sigma}{dk}\right)_{\text{D}} dk,$$

$$\text{B: } \sigma = \langle w_s \rangle \langle w_k \rangle \int_0^1 \left(\frac{d\sigma}{dk}\right)_{\text{D}} dk. \tag{5.15}$$

The two formulae correspond to methods A and B of implementing spin effects and they result from general rules given in Section 4.

Other applications

The methods presented in this Section generalize to higher spins and to sequential (cascade) decays. For example the presented IAMC methods of dealing with spins of $e^{\pm}$ and $\tau^{\pm}$ generalize easily to $e^+e^- \to W^+W^-(\gamma)$, $W^{\pm} \to X^{\pm}$ process. In this case a straightforward extension of the method B may be based on a dominant distribution

$$d\sigma_D \simeq R_{0000}^{00} d\tau_{prod} H_{(1)0}^{0} d\tau_{dec}^{(1)} H_{(2)0}^{0} d\tau_{dec}^{(2)} \tag{5.16}$$

and a generalization of the method A to this process is also possible.

Another example is the process

$$e^+e^- \to \tau^+\tau^-(\gamma), \quad \tau^+ \to X^+, \quad \tau^- \to \nu\varrho^-, \quad \varrho^- \to \pi^-\pi^0, \tag{5.17}$$

comprising a sequential decay of τ^- [14, 38]. In this case the d.c. section may be written, see also Appendix A, as follows:

$$d\sigma = \sum_{abcd} \sum_{J=0}^{2} \sum_{M=-J}^{J} \tilde{\varepsilon}_{(1)}^{a} \tilde{\varepsilon}_{(2)}^{b} R_{abcd} d\tau_{prod}$$

$$\times H_{(1)}^{c} d\tau_{dec}^{(1)} H_{(2)M}^{d\ J} d\tau_{dec}^{(2)} W_M^J d\tau_{dec}^{(3)}, \tag{5.18}$$

where $H_{(2)M}^{d\ J}$ is obtained from spin amplitudes for $\tau^- \to \nu\varrho^-$ similarly as in Eq. (2.24), and W_M^J from spin amplitudes for $\varrho^- \to \pi^-\pi^0$ as in Eq. (A.8).

A possible IAMC algorithm for the above process may be designed using an integral $\int d\tau_{dec}^{(2)} W_M^J = \delta_{J0}\delta_{M0}$ as a basis for the API method. First, the process $e^+e^- \to \tau^+\tau^-(\gamma)$, $\tau^+ \to X^+$, $\tau^- \to \varrho^-\nu$ is simulated according to a partially integrated distribution

$$d\sigma^{(1)} = \sum_{abcd} \sum_{JM} \tilde{\varepsilon}_{(1)}^{a} \tilde{\varepsilon}_{(2)}^{b} R_{abcd} d\tau_{prod} H_{(1)}^{c} d\tau_{dec}^{(1)} H_{(2)0}^{d\ 0} d\tau_{dec}^{(2)}, \tag{5.19}$$

using any of the two methods (A or B) discussed earlier in this Section, and then the decay of ϱ^- is generated using RT based on a dominant distribution obtained from (5.18) by substitutions $J = 0$, $M = 0$.

In the production part $e^+e^- \to \tau^+\tau^-(\gamma)$, a possible future development will be the use of spin amplitudes in generating $d\sigma/d\tau_{prod}$. So far it has not been necessary (only w_s is calculated using the ANSA method), but it may appear to be necessary (or profitable) when the Z_0 is included (at higher s) in a full resonance form.

6. Summary and conclusions

In this paper I review the techniques used in analytical and numerical calculations of the $O(\alpha^3)$ QED distributions for the combined τ production and decay process in e^+e^- scattering at the PETRA/PEP energy range. A particular emphasis is put on spin effects and on Monte Carlo techniques in the numerical calculations.

This work may be treated as a useful supplement to Refs [10] and [11], elucidating many technicalities there, but its other aim was to prepare the ground for other future applications and extensions of the methods which have been used in those works.

In practical terms, the M.C. program of Ref. [11], where most of the technical developments discussed here were used, may be used for the following process:

(A) The process $e^+e^- \to \tau^+\tau^-(\gamma)$, $\tau^\pm \to X^\pm$, from τ production threshold to the highest PETRA energies ($\sqrt{s} \sim 45$ GeV); With some caution (no Z_0 exchange in the hard bremsstrahlung part), it may also be used for e^+e^- annihilation into u, d, s, c, b quark pairs.

The possible future developments and applications may be grouped in three classes as follows:

(B) The processes $e^+e^- \to \tau^+\tau^-(\gamma)$, $\tau^\pm \to X^\pm$ and $e^+e^- \to \bar{q}q(\gamma)$, $\bar{q}q \to$ jets; $m_\tau, m_q \ll \sqrt{s}/2$, 40 GeV $\lesssim \sqrt{s}$. The Z_0 exchange has to be included here, both in soft and hard bremsstrahlung parts, in a full resonance form. The smallness of the τ or quark mass simplifies here the calculations of spin amplitudes and distributions, and the spin structure in the IAMC algorithm.

(C) The process $e^+e^- \to \bar{q}q(\gamma)$, $\bar{q}q \to$ jets, $q = b, t, \ldots$; 40 GeV $\lesssim \sqrt{s}$ $(2m_q \leqslant \sqrt{s})$; Here in addition to Z_0 exchange, one has to keep the finite quark mass which includes a significant algebraic complexity for the $O(\alpha^3)$ QED d.c. sections. The production of a new heavy, spin 1/2, lepton pair also falls into this class.

(D) The production of other heavy, unstable, and (possibly) spin-carrying, particles in e^+e^- scattering processes not far from threshold. A good example is the process $e^+e^- \to W^+W^-(\gamma)$, $W^\pm \to X^\pm$.

Which of the discussed methods may find applications to what processes? The general methods of constructing IAMC algorithms described in Section 4 apply to processes in all classes, A–D, and to any other QED/STPI processes, especially if there are three or more particles in the final state. The specialized IAMC methods of Section 5 (for the τ production part) will find a direct application to processes mediated by the s-channel annihilation i.e. in class B and C.

The presented methods of dealing with spin are also quite general. The techniques of implementing spin effects in the IAMC algorithm discussed in Section 5 apply to the production of any heavy unstable spin-carrying objects i.e. in class A, C and D. The simplifications due to the small mass of spin 1/2 fermions discussed briefly in Section 5 may be used in class B and generally for initial state e^+e^- beams (in the absence of the $e^\pm$ transverse polarizations).

The use of spin amplitudes was advocated in order to reduce the algebraic complexity of the calculations; this is achieved by a numerical evaluation of the d.c. sections from spin amplitudes (ANSA technique, see Introduction). That method was used indeed, see Section 5 and Refs [10, 11], for processes of class A; it will also be useful in classes B, C, D and for other processes. Using ANSA techniques is necessitated either by the presence of spin effects in the final state (spin sensitive decay of $\tau^\pm$, $W^\pm$), or by mass effects, and a multi-

tude of Feynman diagrams, class C and D. If such methods, for any reasons, are already used then introducing spin polarizations for incident ($e^{\pm}$) beams becomes rather trivial.

The methods of defining spin states and calculating spin amplitudes demonstrated in Sections 2 and 3 apply directly to classes A, B and C and they generalize also to other QED processes.

One subject, the discussion of the numerical results from the M.C. calculations illustrating the importance of the QED $O(\alpha^3)$ radiative corrections and of spin effects, was omitted here. It was discussed extensively, however, in Ref. [10] and a short review of these results may also be found in Ref. [39]. As expected, the $O(\alpha^3)$ radiative corrections to the $e^+e^- \to \tau^+\tau^-$ process are rather similar in character to those in $e^+e^- \to \mu^+\mu^-$. They modify the integrated cross section by up to 30% and the angular distributions by typically 10% (depending on cut-offs). The QED induced polarization of the τ is rather small ($\lesssim 1\%$). The effects due to spin correlations (even for unpolarized $e^{\pm}$) are present also in the lowest order [13], and they produce effects of order 5–25% (depending on cut-offs and τ decay mode). These spin effects remain essentially the same when radiative corrections are switched on. It is clear, from these results, that spin and radiative effects are of similar order, and should be taken into account simultaneously. Z_0 exchange induces an angular asymmetry and small τ polarization which, when measured, may provide valuable information on the Z_0 vector coupling constant to the lepton τ.

The exchange of the electroweak boson Z_0 was taken in Refs [10, 11] in the low energy (far from the pole) approximation, suitable in the $\sqrt{s} \ll M_Z$ region, and in Refs [29, 31] it is added to QED, somehow ad hoc, as an additional massive vector boson with coupling constants and a mass being free (adjustable) parameters. The main effort in those works went into mastering the QED hard and virtual bremsstrahlung effects. This approach is justified by the fact that genuine "non-QED" radiative effects coming from the complete calculations of the $O(\alpha^3)$ radiative corrections in the Standard Electroweak Theory [2, 6] are usually rather small [40, 41, 42]. If later the calculations of such corrections are available, in a form suitable for M.C. calculations, then they may be implemented in a M.C. program including pure QED effects rather easily, by an additional rejection. In fact a program of this class would be very helpful in extracting such interesting effects from the precise experimental data, providing eventually experimental evidence for the renormalizability of the Standard Model.

Summarizing, I believe that this work, together with results of Ref. [10] and the M.C. program of Ref. [11], will be useful in data analysis of the τ pair (and heavy quark) production data at the PETRA/PEP energy range. On the other hand it provides a good starting point for many applications to other processes in e^+e^- scattering at higher (SLC/LEP) energies.

The author is grateful to prof. F. A. Berends for encouragement to start the investigation of the radiative corrections to heavy fermion production, to dr. Z. Wąs for invaluable assistance and cooperation in many stages of this work and to dr. R. Kleiss, dr. C. Kiesling and prof. A. Kotański for useful discussions.

APPENDIX A

The decomposition of the density matrix, for spin $s = 1/2$ particle

$$\varrho = \tfrac{1}{2}(1+\vec{\sigma}\cdot\vec{w}), \tag{A.1}$$

where $\vec{w} = 2\langle\vec{S}\rangle = 2\mathrm{Tr}(\varrho\,\vec{S})$ is the polarization vector, generalizes to higher spins as follows [39]

$$\varrho_{mm'} = \sum_{J=0}^{2s}\sum_{M=-J}^{J} T_M^J Z_{M,mm'}^J, \tag{A.2}$$

where

$$Z_{M,mm'}^J = (-)^{J-s-m}\langle s, -m, s, m'|JM\rangle, \tag{A.3}$$

and the polarization vector is closely related to T_M^1:

$$\begin{aligned} T_0^1 &= c_s\langle S_z\rangle, \\ T_{\pm 1}^1 &= \mp c_s 2^{-1/2}\langle S_x \pm iS_y\rangle, \\ c_s &= 3^{1/2}((2s+1)(s+1))^{-1/2}. \end{aligned} \tag{A.4}$$

The elements T_M^J characterize ϱ in a complete way similarly as $\vec{w}$ for $s = 1/2$.

Double spin indices may be converted to $\binom{J}{M}$ notation also for any unstable intermediate particle. The differential cross section

$$d\sigma \simeq \sum_{\lambda\lambda'} \mathcal{M}_\lambda(\mathcal{M}_{\lambda'})^* T_\lambda(T_{\lambda'})^* d\,\mathrm{lips}, \tag{A.5}$$

where $\mathcal{M}_\lambda$, $\lambda = -s \ldots s$ are spin transition amplitudes for the production process and T_λ for the decay process, may be rewritten using a completeness identity

$$\sum_{JM} Z_{M,\lambda\lambda'}^J Z_{M,\mu\mu'}^J = \delta_{\lambda\mu}\delta_{\lambda'\mu'}, \tag{A.6}$$

as follows

$$d\sigma \cong \sum_{JM} R_M^J W_M^J d\,\mathrm{lips}, \tag{A.7}$$

where

$$\begin{aligned} R_M^J &= \sum_{\lambda\lambda'} \mathcal{M}_\lambda(\mathcal{M}_{\lambda'})^* Z_{M,\lambda\lambda'}^J, \\ W_M^J &= \sum_{\lambda\lambda'} T_\lambda(T_{\lambda'})^* Z_{M,\lambda\lambda'}^J. \end{aligned} \tag{A.8}$$

Let us take the example of $e^+e^- \to \tau^+\tau^-$, $\tau^+ \to X^+$, $\tau^- \to \varrho^-\nu$, $\varrho^- \to \pi^0\pi^-$ process. In this case

$$\begin{aligned} d\sigma \sim \sum_{J_i M_i} & T_{(1)M_1}^{J_1} T_{(2)M_2}^{J_2} R_{M_1 M_2 M_3 M_4}^{J_1 J_2 J_3 J_4}(e^+e^- \to \tau^+\tau^-(\gamma)) d\tau_{\mathrm{prod}} \\ & \times H_{(1)}(\tau^+ \to X^+)_{M_3}^{J_3} d\tau_{\mathrm{dec}}^{(1)} H_{(2)}(\tau^- \to \varrho^-\nu)_{M_4 M}^{J_4 J} d\tau_{\mathrm{dec}}^{(2)} W_M^J(\varrho^- \to \pi^-\pi^0) d\tau_{\mathrm{dec}}^{(3)}. \end{aligned} \tag{A.9}$$

The above formula is almost identical to that of Eq. (5.17). The only difference is that for

$s = 1/2$ fermions the Cartesian indices $a = 0, 1, 2, 3$ are used instead of polar ones $\begin{pmatrix} J \\ M \end{pmatrix} = \begin{pmatrix} 0 \\ 0 \end{pmatrix}\begin{pmatrix} 1 \\ -1 \end{pmatrix}\begin{pmatrix} 1 \\ 0 \end{pmatrix}\begin{pmatrix} 1 \\ -1 \end{pmatrix}$. The relation between them is easily deduced from the expansion

$$Z_0^0 = 2^{-1/2}\sigma_0, \quad Z_0^1 = 2^{-1/2}\sigma_3, \quad Z_{\pm 1}^1 = 2^{-1}(\mp\sigma_1 + i\sigma_2), \tag{A.10}$$

see also Eq. (A.4). The angular distributions $W_M^J(\varrho^- \to \pi^-\pi^0)$ are in fact proportional to spherical harmonics $Y_M^J(\theta, \varphi)$, where θ, φ are the polar angles of the π^- in the ϱ^- rest frame, for more details see Refs [18, 43, 44].

REFERENCES

[1] C. N. Yang, R. L. Mills, *Phys. Rev.* **96**, 191 (1954).

[2] S. L. Glashow, *Nucl. Phys.* **22**, 579 (1961); S. Weinberg, *Phys. Rev. Lett.* **19**, 1264 (1967); A. Salam, Proc. of 8-th Nobel Symposium 1968, ed: N. Svartholm, 367, Wiley 1968; S. L. Glashow, J. Iliopulos, L. Maiani, *Phys. Rev.* **D2**, 1285 (1970).

[3] H. Fritzsch, M. Gell-Mann, Proc. XVI Int. Conf. on High Energy Physics, Chicago, Vol. 2, 135 (1972).

[4] F. E. Close, *An Introduction to Quarks and Partons*, Academic Press, 1979.

[5] Sau Lan Wu, e^+e^- Physics at PETRA — the first five years, DESY 84-028 preprint, to be published in *Phys. Rep.*; G. Wolf, High energy e^+e^- interactions, DESY 81-086 preprint.

[6] G. 't Hooft, *Nucl. Phys.* **B33**, 173 (1971); **B35**, 167 (1971).

[7] F. M. Renard, Basics of electron-positron collisions, Edition Frontières, Gif sur Yvette 1981.

[8] C. F. v. Weizsäcker, *Z. Phys.* **88**, 612 (1934).

[9] F. James, FOWL, A general Monte-Carlo phase space program, CERN Program Library, W505, (1970); W. Kittel, W. Wójcik, L. Van Hove, *Comput. Phys. Commun.* **1**, 425 (1970); S. Jadach, *Comput. Phys. Commun.* **9**, 237 (1975).

[10] S. Jadach, Z. Wąs, *Acta Phys. Pol.* **B12**, 1151 (1984) and Erratum *Acta Phys. Pol.* **B16**, 483 (1985).

[11] S. Jadach, Z. Wąs, *Comput Phys. Commun.* **36**, 191 (1985).

[12] M. I. Perl et al., *Phys. Rev. Lett.* **35**, 1489 (1975); M. I. Perl, *Ann. Rev. Nucl. Part. Sci.* **30**, 299 (1980).

[13] Y. S. Tsai, *Phys. Rev.* **D4**, 2821 (1971).

[14] H. Kühn, F. Wagner, *Nucl. Phys.* **B236**, 16 (1984).

[15] H. J. Behrend et al., *Phys. Lett.* **127B**, 270 (1983); H. J. Behrend et al., DESY 84-020 preprint, to appear in *Phys. Lett.*

[16] R. Kleiss, *Nucl. Phys.* **B241**, 61 (1984).

[17] F. A. Berends, R. Kleiss, P. H. Davernveldt, Complete Lowest Order Calculations for Four Lepton Final States in Electron-Positron Collisions, Leiden University preprint 1984.

[18] M. Jacob, G. C. Wick, *Ann. Phys.* **7**, 404 (1959); Suh Urk Chung, Spin Formalism, CERN report 71-8 (1971).

[19] F. A. Berends, R. Kleiss, P. de Causmaecker, R. Gastmans, T. T. Wu, *Phys. Lett.* **103B**, 124 (1981).

[20] F. A. Berends, R. Kleiss, P. de Causmaecker, R. Gastmans, W. Troost, T. T. Wu, *Nucl. Phys.* **B206**, 61 (1981).

[21] P. de Causmaecker, R. Gastmans, W. Troost, T. T. Wu, *Phys. Lett.* **105B**, 215 (1981); *Nucl. Phys.* **B206**, 53 (1982).

[22] J. D. Bjorken, S. D. Drell, *Relativistic Quantum Mechanics*, Mc Graw-Hill, New York 1964.

[23] B. Lautrup, RIWIAD, Proc. 2-nd Colloquium on Advanced Computing Methods in Theoretical Physics, Marseille 1971.

[24] G. P. Lepage, VEGAS, *J. Comput. Phys.* **27**, 192 (1978).

[25] C. J. Everett, E. D. Cashwell, A Monte Carlo Sampler, Los Alamos Scientific Laboratory Informal Report ANL/ES-26 (1972).
[26] R. Kleiss, Monte Carlo Simulation of Radiative Processes in Electron-Positron Scattering, Ph. D. Thesis, Leiden University 1982.
[27] F. James, *Rep. Prog. Phys.* **43**, 1145 (1980).
[28] T. M. Hamersley, D. C. Handscomb, *Monte Carlo Methods*, Methuen, London 1964.
[29] F. A. Berends, R. Kleiss, *Nucl. Phys.* **B177**, 237 (1981).
[30] F. A. Berends, R. Kleiss, S. Jadach, Z. Wąs, *Acta Phys. Pol.* **B14**, 413 (1983).
[31] F. A. Berends, R. Kleiss, S. Jadach, *Nucl. Phys.* **B202**, 63 (1982).
[32] F. A. Berends, R. Kleiss, S. Jadach, *Comput. Phys. Commun.* **29**, 185 (1983).
[33] F. Bloch, A. Nordsieck, *Phys. Rev.* **52**, 54 (1937).
[34] D. R. Yennie, S. Frautschi, H. Suura, *Ann. Phys.* (N.Y.) **13**, 379 (1961).
[35] S. Jadach, Monte Carlo Simulation of Deep Inelastic ep → epX Scattering, in preparation.
[36] G. Altarelli, G. Parisi, *Nucl. Phys.* **B126**, 298 (1977).
[37] F. A. Berends, R. Kleiss, *Nucl. Phys.* **B178**, 141 (1981).
[38] J. E. Brau, G. J. Tarnopolsky, *Phys. Rev.* **D24**, 2521 (1981).
[39] Z. Wąs, *Acta Phys. Austriaca*, Suppl. XXVI, 447 (1984).
[40] W. Wetzel, Electro-Weak Radiative Corrections for $e^+e^- \to \mu^+\mu^-$ at PETRA Energies, University of Heidelberg preprint, May 1983.
[41] W. Hollik, Weak Corrections to Polarization and Charge Asymmetries in $e^+e^- \to \mu^+\mu^-$ Around Z_0, DESY 84-075 preprint.
[42] M. Böhm, A. Denner, W. Hollik, R. Sommer, Radiative Corrections to Bhabha Scattering in $SU(2) \times U(1)$, DESY 84-040 preprint.
[43] A. Kotański, Resonance Decay Distributions..., lectures in Herceg-Novi School 1970.
[44] A. Kotański, K. Zalewski, *Nucl. Phys.* **B4**, 559 (1968).